2007

A general material removal strategy based on surface sampling and reconstruction on unknown objects

Danni Wang
Iowa State University

A general material removal strategy based on surface sampling and reconstruction on unknown objects

by

Danni Wang

A dissertation submitted to the graduate faculty

in partial fulfillment of the requirements for the degree of

DOCTOR OF PHILOSOPHY

Major: Industrial Engineering

Program of Study Committee:
Frank E. Peters, Co-major Professor
Matthew C. Frank, Co-major Professor
Sigurdur Olafsson
Leonard S. Chumbley
Palaniappa A. Molian

Iowa State University

Ames, Iowa

2007

TABLE OF CONTENTS

ABSTRACT

In most material removal processes, the size and shape of the stock material, the desired surface and the orientation of the part are known. If some or all of these factors are unknown, typical automatic systems will not be able to handle the situation. In reality, most of these cases are subsequently handled by human operators. This results in low productivity and inconsistency in the production and potential ergonomic problems for the human operators. Therefore, a new system needs to be designed to meet the requirements for material removal with unknown objects.

This dissertation presents a feasible and efficient automatic system for material removal with unknown processing factors. The characteristics of this type of processes were investigated. The corresponding inputs of the system were decided, while balancing the ease of use and the complexity of the system. A simple point sampling strategy was developed to sample the reference points, which are used to create the approximated surface for the unknown objects with a modified triangular based surface approximation method. A universal layer based path planning method was developed to guide the tool among the layers within the designated working area to remove the excess material effectively and efficiently without changing the programming codes.

This system was verified by simulations and a prototype of the grinding system.

CHAPTER 1. GENERAL INTRODUCTION

1.1 Introduction

Material removal processes are very common in modern manufacturing. Most of the common material removal processes are conducted where the amount and location of the material to be removed is known beforehand. An example of this is CNC machining. The stock size, the orientation and the position of the stock and the part, and the CAD model of the part are all known and therefore a fixture can be used to maintain the correct position. In this case, path planning can be made in advance and simulations can be done to check the final result. If the simulation result is accepted, corresponding machining codes will be generated and sent to the machine and the part can be created automatically and precisely.

However, there are a number of material removal processes whereby not all the information given above is known. An example is the post shakeout material removal operations for metalcastings. The locations, size and shape of the excess material to be removed are different for each casting even though they are made from the same pattern. In this type of material removal process, a normal automatic system is often not feasible and the material removal is done via tedious manual processes such as hand grinding. Manual operations can take advantage of an intelligent operator with experience and be very flexible. However, humans can also be inconsistent and less efficient. In addition, there are significant

ergonomic issues associated with having a human operator remove large amounts of metal via hand grinding.

This dissertation focuses on material removal processes with unknown objects; a general material removal strategy for this type of material removal process is proposed. The general goal is to create methods for having an automated machine to supplement the skill and flexibility of a human operator. More specifically, this dissertation will focus on the grinding of metalcastings.

Most metalcastings require some grinding after they are shaken out of the molds, done in an area commonly called the cleaning room. This grinding is used to remove the riser and gating contacts, possibly smooth the parting line, and correct any other surface anomalies such as burnt on sand. For castings that are upgraded by welding, grinding is used to blend these surfaces as well.

Other than a few special cases, all cleaning room grinding in steel foundries as well as low production cast iron products is performed by operators manually manipulating the grinder. Figure 1-1 shows some anomalies on castings that need to be manually removed. The operators must apply effective force on complex shaped castings, which is a significant ergonomic problem because of the force required, poor position, and vibration. Among other issues, this results in high job turnover and a wide variation in grinding processing time. Some castings are over ground, leading to a waste of time and energy, while some are not ground sufficiently, leading to rework.

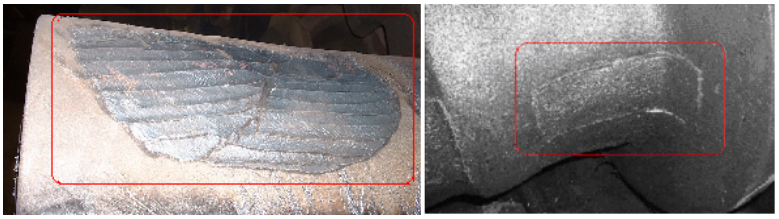

Figure 1-1 Some example anomalies

The material removal process of cleaning room grinding has the following characteristics.

- **Unknown orientation:** Customized fixturing for each casting cannot be justified because of the low volume and product diversity. Therefore, the orientation of each part varies.

- **Unknown locations:** Because of the variability in the casting process, each casting is different and therefore the locations that need to be ground are unknown. This is in addition to the expected grinding such as the grinding of parting lines and risers.

- **Unknown desired surface:** The CAD data of the casting may be given, but since the orientation of the casting is unknown, it is difficult to transform the CAD model from its coordinate system to the machine coordinate system.

- **Unknown anomalies:** The shape and size of the anomalies are irregular and unpredictable due to the variability in the metal casting process. The amount of material to be removed from each location on each casting is different.

- **Relatively low precision:** The main goal of cleaning room grinding is to remove extra material and make the surface smooth. Cleaning room grinding has a larger tolerance than surface grinding. Surface grinding can be as precise as 0.001 inches (0.0254 mm), while the tolerance for cleaning room grinding is often on the order of 0.1 inches (2.54 mm).

- **Large range of product sizes:** The weight range of the castings is from 1 to 100,000 pounds (0.45 to 45,000 kgs).

Grinding robots and automated machines are widely used to grind the expected locations on medium and high volume castings. However, current automation solutions are

not feasible for lower volume products. In order to grind on a different type of casting, changes must be made to the program, the fixture and the machine itself. It takes great time and effort to design the fixture, plan the path and tooling and set up the machine for current automatic devices. The steel casting industry produces a wide variety of lower volume products. It is not feasible to construct fixtures that would facilitate the use of robots to accommodate this product diversity. Furthermore, unlike grinding gating and riser contacts in which the location is known, the location of other geometric anomalies on the surface of the part is unknown. Even the size of the anomaly at known locations will vary significantly making it difficult for a fixed automation cycle. Therefore, an automatic material removal approach that is significantly different than the available grinding robots is needed.

The general material removal strategy must be able to deal with the unknowns listed above, and the machine should meet the following requirements:

- **Flexible:** The machine should be able to work on any arbitrary surface without "knowing" the real geometric data of the objects. The system shall not require any software or hardware changes for different types or sizes of objects or a different surface.

- **Autonomous:** Other than entering some initial inputs, it should be able to guide itself without human input and control. An appropriate path and suitable force should be calculated and real-time adjustments should be made according to the initial input and feedback system. This allows the machine to run unattended. The machine would need to detect and avoid dangerous conditions such as applying excessive force.

- **Consistent quality:** The machine needs to constantly perform high quality.

1.2 Dissertation organization

Chapter 1 introduces the material removal problem on unknown objects and its characteristics. Chapter 2 provides a general literature review of this problem. Chapter 3 gives the overview of the proposed solution. Chapter 4 focuses on the points sampling and surface approximation methods which is part of the proposed solution. Chapter 5 presents a novel path planning method for the material removal on unknown objects which is another part of the proposed solution. Chapter 6 completes the solution, demonstrates the implementation methods and provides a prototype to the proposed system and testing results. Chapter 7 gives the conclusion of this dissertation and future work.

CHAPTER 2. LITERATURE REVIEW

There has been considerable research on removing material with a robotic manipulator. Some of the literature on robotic grinding discussed ways to control the grinding force, plan the path and improve the surface grinding qualities (Pagilla 2001; Erlbacher 2000; Wang 2000; Thomessen 2001; Dimo 2001). These approaches depend on CAD data and are not flexible enough to handle the unexpected material removal such as the grinding required in many metalcasting applications. Nandi (2004) and several researchers have tried to add intelligence to the machines, but their efforts were made to find better strategies to grind on a known structure.

Other researchers have studied the position and force control with unknown surfaces and unknown environmental variables such as stiffness. Impedance force control and hybrid force/position control are two broad force control approaches (Yoshikawa 2000). Impedance control assumes that there is a prescribed static or dynamic relation between the applied force and the position. When in contact with the environment, the mechanical impedance of the end effecter is adjusted to high if achieving the desired position is the priority and to low if the compliance to the external force is preferred (Hogan 1985). In hybrid control, the force is controlled in selected directions and the position control is used in complementary directions (Raibert 1981); there are usually two separate feedback loops for both the position and the force, and a joint actuator will follow the correction signals to guide the manipulator along

the desired position trajectory while applying proper force. Jung (2004) used impedance control to determine the desired force in an unknown environment, while Yin (2004) used fuzzy hierarchical coordination and neural control. Kuo(1997) and Kiguchi (2000) used fuzzy neural networks to find the real force direction from the noisy signals. Roy (2002) presented an adaptive force controller for position/velocity controlled robots in contact with surfaces of unknown linear compliance. Iwasaki (2003) developed a new type of sliding mode controller with gain-scheduled variable hyper plane for position and force control, which can be continuously adjusted according to the environmental stiffness identified in real time. Much of these works was directed at surfaces the geometry of which remains unchanged. In contrast, the material removal process discussed in this dissertation needs to remove a variable amount of material at variable locations, which makes the part quite different from the desired geometry.

Chen (2000) used an innovative geometrical projection method to plan the trajectory for automated robotic deburring on an unknown contour. It used a force sensor to detect the tangent direction of the real trajectory and hence to plan the next target position based on transforming a segment of a predefined circular trajectory to a segment of the true trajectory. This deburring process did change the geometry of the unknown objects, but this work was only done with curves/contours, not with surfaces.

Previous work is related to the material removal process on unknown objects to some extent, however, the literature indicates little research on this problem, and none considering the specific problem stated in this dissertation.

CHAPTER 3. SYSTEM STRUCTURE

The greatest difficulty in material removal with unknown objects is the lack of information about the object such as the locations of the anomalies. A vision system is not feasible because it cannot identify anomalies, especially in the environments that the systems need to operate within. Another option is to ask the operator to instruct the machine where to work on each part, and then the machine will guide the tool throughout the indicated areas while applying the desired force automatically.

The system flow is shown in Figure 3-1. A human operator is needed to inspect the part for the anomalies, and decide which mode should be used for material removal on this particular part.

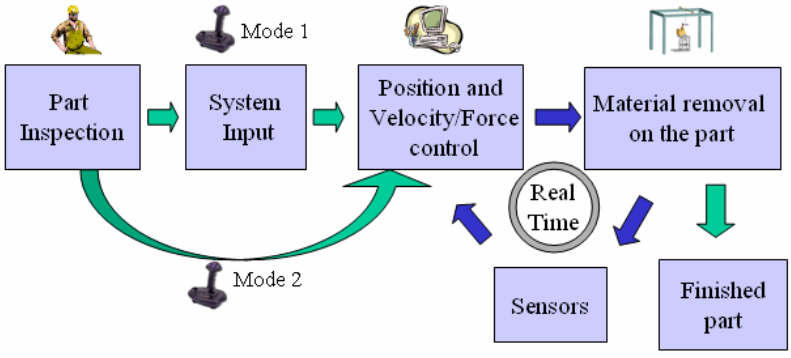

Figure 3-1 System flow

Mode 1) Automatic mode: With appropriate inputs, the computer can take control of both path planning, position and velocity/force control to work in the designated area automatically. When all the anomalies in this area have been adequately removed, the machine will move the tool to the machine home.

Mode 2) Manual mode: If conditions don't warrant the use of the automatic mode, the operator can handle the position control via a joystick, while the machine will

maintain a constant velocity (i.e. feed rate) and a constant force on the parts. In this mode, the operator acts as the path planner and the position controller, while the control algorithms maintain force application.

There is considerable unknown information in material removal processes with unknown objects. It is impossible to get the work done without any information at all, so the problem becomes to construct an automatic system that can remove the excess material automatically with minimum inputs. The required information varies for each case, with some situations needing more inputs than simpler ones. For example, a slot totally covered by the anomaly will need the original drawing to find out its dimension and location. This information cannot be acquired only by inspecting the part with the anomaly. It is critical to balance the flexibility and the complexity of the system, so assumptions are made to define the required inputs that will fit most cases in the metalcasting industry. For those parts that need more information than the required inputs, and those whose required inputs are not available, an alternative manual mode is proposed as a system addition to further assist the material removal process. The development of the manual system is not detailed here.

For an automatic system with so much unknown information, the first challenge is to design proper system input variables to balance the flexibility of the system and the complexity of the inputs. Assumptions are made to simplify the system, sacrificing the flexibility of the automatic process, leaving all the situations that cannot be automated to the manual mode.

The unknown orientation, unknown locations, unknown desired surface and unknown anomalies described in Chapter 1 are handled differently to fit the automatic system.

3.1 Handling Unknown Orientation

Because it is not practical to fixture for all castings to be processed, it is impossible to fix the castings in a specific orientation. Therefore, there is no way to determine the transformation matrix of the part from its coordinate system in the CAD model to the machine coordinate system, and the algorithm for the automatic process must be able to work without knowing it. However, the casting must be held in place during the material removal process so that it won't move. To assure accessibility, an assumption is made that the casting will be oriented such that the anomalies are facing up (Figure 3-2).

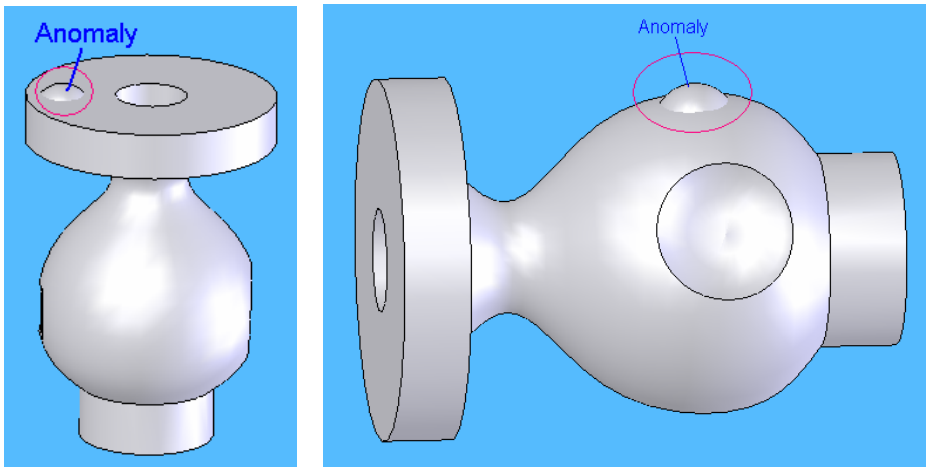

Figure 3-2 Parts positioned to have the anomalies facing up

The angle between the grinding wheel axis and the part will affect the surface finishing result. It is not trivial to calculate the optimal angle, even if the CAD model of the casting and the orientation of the casting are given. In an automated system with limited inputs,

changing this angle during grinding may cause unexpected exceptions. Therefore, once the part is anchored in the system, a rotation angle θ of the grinding wheel axis in the machine coordinate system is given so that the grinder can access the part and maximize the width of the wheel that is in contact with the surface. This angle is also used to define the working coordinate system by rotating the machine coordinate system around the Z axis by θ degrees (Figure 3-3). In the working coordinate system, the X_w axis is parallel to the axis of the grinding wheel, the Y_w axis is in the plane of the grinding wheel, and the origin of the coordinate remains the same as that of the machine coordinate system. Grinding is to be performed primarily along the Y_w axis, with feed in the X_w direction.

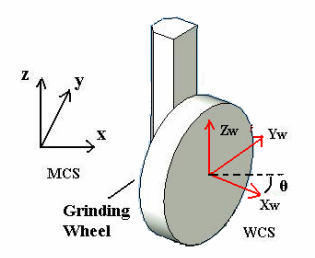

Figure 3-3 The rotation angle between Machine and Working Coordinate Systems

3.2 Inputting the Anomaly Locations

The grinding locations can vary for each casting, so they have to be manually input into the system. It is straightforward to use a set of boundary points $\{b_i\}$ to mark the area to be ground. The set of points $\{b_i\}$ is projected to the X-Y plane of the working coordinate system to form the anomaly boundary polygon B, which will be used as the cross section of a prism within which grinding will be performed. There can be multiple anomalies within the

boundary defined by the set of boundary points $\{b_i\}$. The automatic system will and should only work in the region defined by this boundary.

3.3 Approximating the Desired Surface

The desired surface can potentially be found from the CAD data, but it is impossible to transform the model from its coordinate system to the machine coordinate system since the orientation of the casting is unknown. So points need to be sampled from the part surface to generate an approximation of the desired surface. Another set of boundary points $\{s_i\}$ is used to indicate the area within which good surface points can be sampled to create the approximated surface beneath the anomalies. The $\{s_i\}$ boundary points are projected to the X-Y plane of the working coordinate system to form the sampling boundary polygon S. (Figure 3-4)

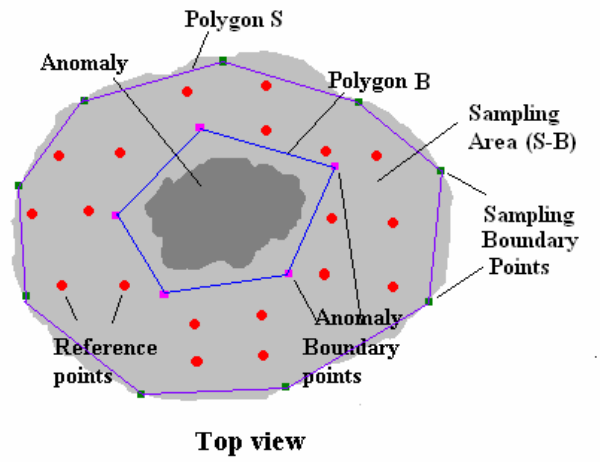

Figure 3-4 Anomaly boundary points, sampling boundary points and reference points

The reference points are points sampled on the smooth (good) surface of the casting within the sampling area defined by *(S-B)* outside the anomaly area. The approximated

surface can be derived from the reference points to the entirety of the containment boundary *B*. For planar surfaces, the approximated plane within the anomaly boundary can be calculated from an equation defined by three nonlinear points located anywhere on the surface. For non-planar surfaces, surface approximation methods usually can only calculate the surface points within the convex hull of the sampled points. Surface points outside this convex hull won't be reliable due to insufficient surface information. Therefore, for non-planar surfaces, to assure a better approximated surface within the anomaly boundary, polygon *B* should be inside polygon *S*.

As expected, more points will increase the accuracy of the approximated surface and more complicated surfaces will generally require more data points. For this research, the automatic mode is limited to the following surface patches: planar surface patch, concave surface patch, convex surface patch and saddle surface patch. (Figure 3-5) The method to sample the reference points on these surfaces patches for generating the approximated surface used in the automatic mode will be discussed in chapter 4. For more complicated surfaces, the manual mode will have to be used.

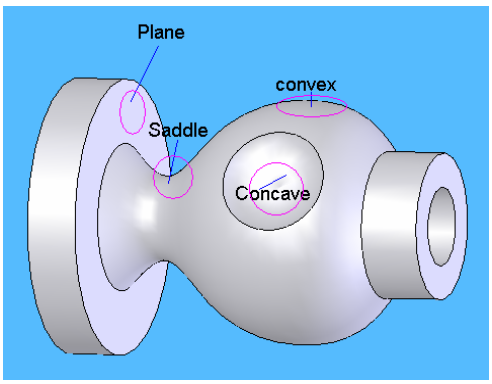

Figure 3-5 Examples of the simple surface patches

Different types of surfaces will need different approximation methods. The surface approximation method selected will affect the way the reference points are sampled. Due to sampling noise, points sampled from a planar surface won't be exactly on a plane, neither will points sampled from a line be exactly linear. So surface type is inputted to the system to tell whether or not the points are designed to be planar/linear. The user needs to specify whether the surface is a plane, a straight swept surface or a free form surface. Surfaces other than plane and straight swept surfaces are all considered free form surfaces because they can be approximated with the same method.

3.4 Handling Anomaly Size and Shape

It is not practical or necessary to get the shape and size of the anomalies because each anomaly is unique and their shape and size are usually unrelated to the desired surface of the part under the anomaly area. The system must be able to automatically handle any anomaly no matter what size and/or shape it is. But to make grinding feasible, it is assumed that the radius of the tool is smaller than the radius of the feature, so that the tool will be able to reach the desired position without digging into the surface.

To summarize, the automatic material removal procedure is shown in Figure 3-6. Initially, the human operator inputs necessary information into the system: the rotation angle θ of the grinder, the desired surface type (planar, straight swept or free-form), one set of anomaly boundary points and one set of sampling boundary points. The computer will take

over the rest of the procedure. First, reference points will be sampled automatically on the good surface within the sampling area defined by the anomaly and sampling boundaries, following the points sampling strategy discussed in chapter 4. Next, an approximated surface (approximation of the desired surface) in the anomaly area is constructed from the reference points, using the methods discussed in chapter 4. Finally, a novel real-time path planning strategy discussed in chapter 5 guides the tool traversing the anomaly boundary according to the approximated surface, searching the anomalies and getting rid of them while maintaining proper cutting force and feed rate.

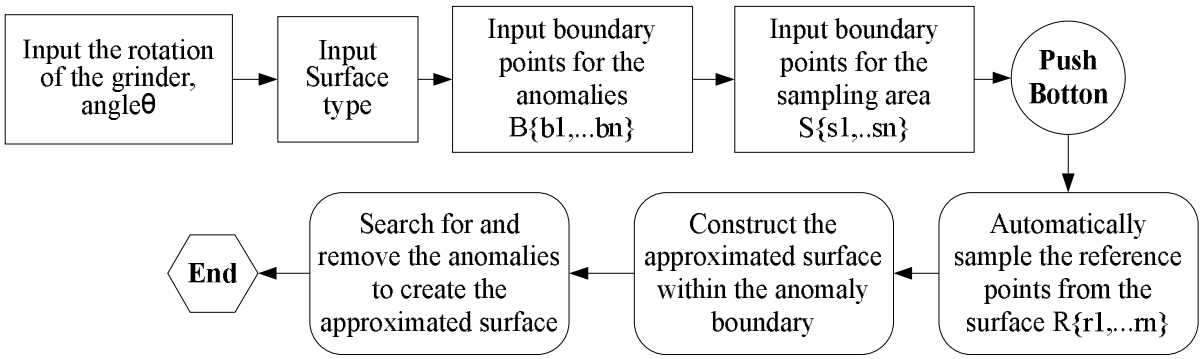

Figure 3-6 The automatic material removal procedure

In this automatic material removal system, the system structure design, surface sampling, approximated surface construction and path planning methods are the main contributions of this dissertation. Methods for position and velocity/force control are well studied in the control fields and will be modified to support the proposed system.

CHAPTER 4. A SIMPLE POINTS SAMPLING STRATEGY FOR UNKNOWN SURFACE PATCH APPROXIMATION

A paper to be submitted

Danni Wang[1], **Frank E. Peters** and **Matthew C. Frank**

Abstract

Points sampling is a very common method used in surface reconstruction. When part of the surface is not available for sampling, and the number of points sampled is limited due to the capability of the sampling device, the points sampling strategy becomes very important in achieving a good approximation of the original desired surface. To solve this problem, three types of surface patches (planar, straight swept and simple free-form) were studied in this paper. A modified Random Mutation Hill Climbing method was used to attain some good sampling sets. Analysis was done to find out the commonality of these sets of sampling points and to form a simple and feasible points sampling strategy for the unknown surface patch approximation.

Keywords: sampling points, estimated points, unknown surface approximation

[1] Primary researcher and author

4.1 Introduction

Points sampling is a very important step in surface reconstruction. In most applications such as reverse engineering, points can be sampled anywhere on the surface to be reconstructed. However, there are some situations in which part of the surface is unavailable for sampling, such as reverse-engineering a damaged part. In the metal casting industry, most metal castings require some grinding after they are shaken out of the molds, done in an area commonly called the cleaning room. This grinding is used to remove surface anomalies such as burnt on sand, gating contacts and parting lines. Since the steel casting industry produces a wide variety of lower volume products from 1 to 100,000 pounds (0.45 to 45,000 kgs), it is not feasible to build fixtures that would facilitate the use of grinding robots to accommodate this product diversity. Since the orientation of the casting is unknown, it is difficult to transform the CAD model from its coordinate system to the machine coordinate system. However, the surface can be approximated from the points sampled on the part surface outside the anomaly area. Points cannot be sampled in the anomaly area since they contain no information about the desired surface beneath the anomalies. The points can be transformed from the coordinate system of the sampling device to the machine coordinate system. This will allow an automatic grinding system to possibly be driven by a surface approximated from the sampling points, rather than the original CAD model.

There are many ways to sample points on a surface, most of which fall in two categories: contact methods and non-contact methods. Contact methods often use a mechanical probe to

touch the surface and record the position when in contact, but the sampling speed is limited because the traveling speed is limited to avoid damage to the probe. Non-contact methods often use lights to measure the distance. While the sampling rate is fast, the performance of the non-contact systems is easily affected by the environmental conditions such as lighting. Appropriate lighting would be extremely difficult to maintain in the industrial environment. Therefore, a mechanical probe is preferred. As it takes longer for a probe to sample points on the surface, a simple sampling strategy with less number of points is preferred. This strategy should also be easy for the human operator or the automatic system to follow.

A lot of research has been done for points sampling and selection. For example, Edgeworth (1999) brought up an adaptive iterative sampling process based on surface normal. Elkott (2002) proposed an automatic sampling strategy for free-form surfaces using heuristics based on the features of the NURBS surfaces. Keith (1996) worked on the optimum sample point selection based on plate deformation theory. Li (2003) used the Fisher information matrix to optimize the sampling location of a free-form surface based on a B-spline model. However, this research was done either with a known surface model or with a surface that can be sampled anywhere (no anomalies in the intended surface). None of the research focused on sampling points on an unknown surface with anomalies to approximate the desired surface beneath the anomalies. Reverse engineering researchers (e.g. Jun 2005) came up with many hole-filling algorithms that are able to interpolate/approximate the surface beneath the anomaly area, but these researches were using hundreds or even

thousands of data points around the hole to generate the surface. It will not be practical to collect that many data points for this application.

This paper introduces a simple points sampling strategy for sampling on surface with anomalies. The strategy will decide how many points to sample (preferably a minimum number) and where to sample these points, with a prediction of the accuracy for the surface approximation. The steel casting grinding scenario is used as an example here.

4.2 Assumptions

Generally speaking, more complicated surfaces will require more data points and result in more complicated issues, such as machining accessibility and tool orientation. The motivation of this research is to find a simple and feasible method that can easily be implemented in an automatic system. Since it is not feasible to have an automated system that can handle any surface, this work is limited to some common surface types: planar surface patches, straight swept surface patches and simple free-form surface patches The straight swept surface patch is created by sweeping a section curve along a straight line. Surface patches other than the planar and straight swept surface patches are considered free-form surface patches. There are three simple free-form surface patches studied in this paper: concave surface patch, convex surface patch and saddle surface patch. Figure 4-1 shows examples of the three simple free-form surface patches.

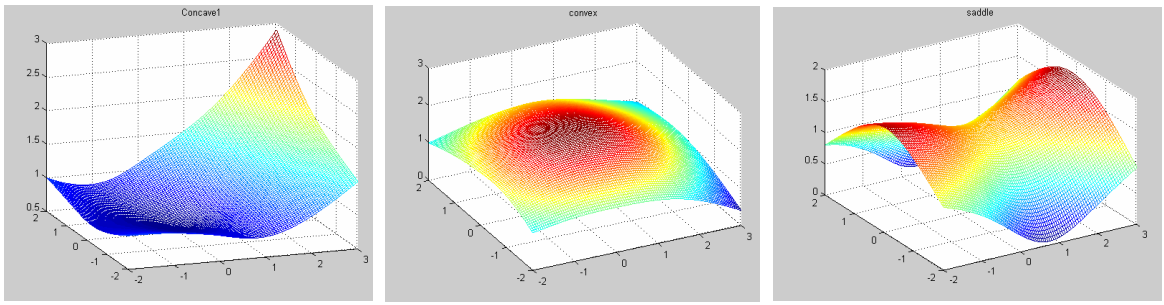

(a) concave (b) convex (c) saddle

Figure 4-1 Three simple free-form surface patches studied in this paper

The following additional assumptions are also made to further limit the complexity:

1) Sample points are collected in an area within which there is only one type of surface patch. Complex surfaces with anomalies should be divided into several regions each of which has only one type of the above surface patches. Since there is no information about the anomalies available before an operator inspecting it, the sampling boundary and the anomaly boundary are inputted into the system by a human operator. Each boundary consists of a sequence of points sampled on the surface patch. The polygon formed by these points is the boundary. Surface area that is within the sampling boundary but not in the anomaly boundary is called the sampling area. (Figure 4-2(a))

2) Each anomaly cannot cross more than one feature of the desired surface. In other words, the points in the sampling area must be able to provide enough information about the desired surface beneath the anomaly. For example, a slot on a cylindrical surface covered by the anomaly couldn't be recovered from the points sampled on the good part of the cylindrical surface. Therefore, the sampling method and surface approximation method in this paper does not include this situation. (Figure 4-2 (b))

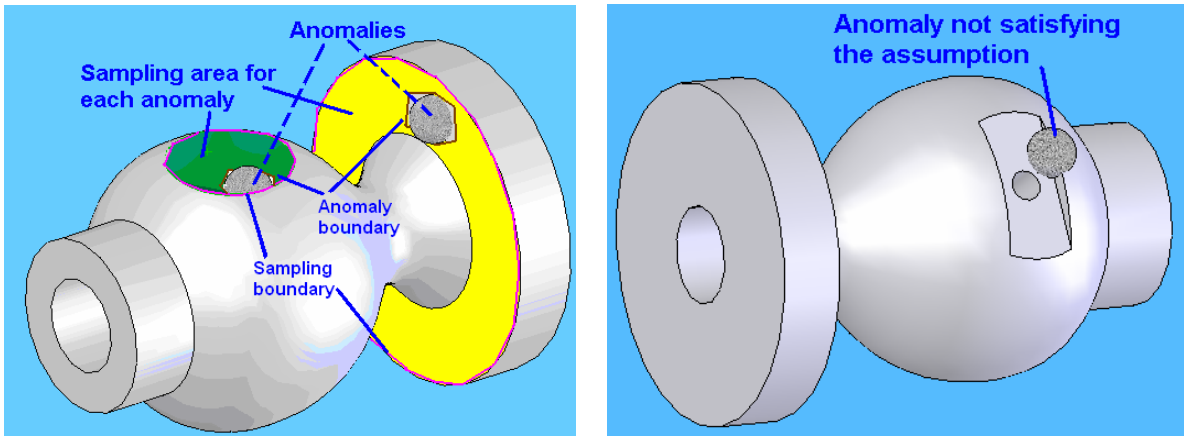

Figure 4-2 (a) Examples of sampling area around various anomalies (b) An example of the anomaly that doesn't satisfy the assumption

4.3 The Surface approximation method

The approximation method must be decided first, because it dictates the sampling strategy.

For planar surfaces, the least square method is used to create an approximation plane that has the least sum of square distance from the sampled points to the approximated plane.

For non-planar surfaces, the straight swept surface patches are separated from the others because they contain straight lines. Points sampled on the same line won't be exactly co-linear due to the measurement error, so the automatic system needs to know whether the non-linear are caused by measurement error or they need to be approximated as a curve. The surface construction method for the straight swept surface is straight forward. First, the line equation will be approximated by a least square means and then a section curve that is in the plane perpendicular to the line is approximated by a cubic spline. The surface patch is calculated by shifting the curve along the line. The cubic spline is used for approximation because it is simple to derive and the cleaning room grinding application has a relatively low surface tolerance (0.1 inches).

The other surface patches require more information to identify, so they will be treated as a free-form surface patch and approximated with the same method.

There are many methods described in the literature for reconstructing a free-form surface from sampled data points. The traditional B-spline approach requires data points in a "grid", which means that points in the same row have the same v value and points in the

same column have the same *u* value, where *u*, *v* are the parameters for the B-spline surface representation (Piegl, 1997). Points cannot be sampled in the anomaly boundary. If point P is in the anomaly boundary, points with the same u/v value as P in the sampling area cannot be used in the B-spline method. Therefore, using the traditional B-spline method will result in a reduction in the available sampling area. (Figure 4-3)

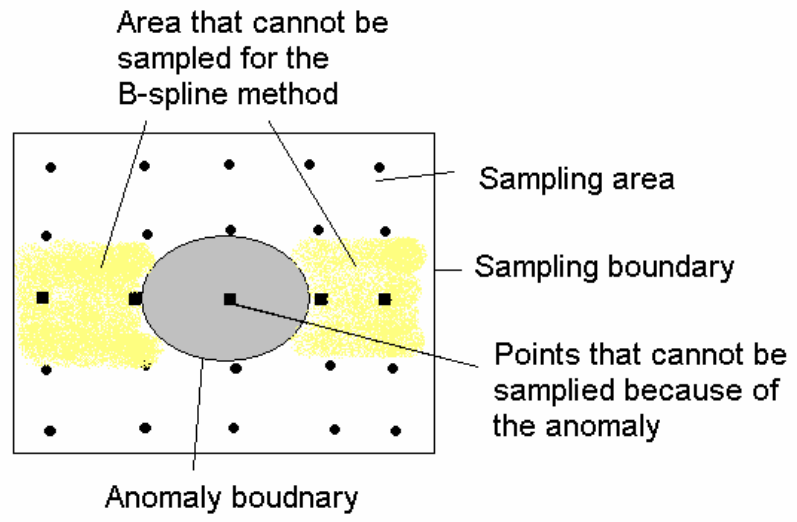

Figure 4-3 The reduced sampling area for the B-spline method

Previous research has been done to modify the traditional B-Spline method, in an attempt to fill in the voids in the anomaly area. Lee (1997) introduced a method to find the z values for the unknown points by assigning 0 to them or by using the z values calculated from the plane fitted from all known points. The shortcoming for this approach is that the fitted plane cannot represent the true surface. The traditional B-spline method can also be modified for use with 3D scattered points. The u and v values of each point can be evaluated from the cord length or centripetal method. Given the degrees on u and v directions, the knot vectors can be calculated from various averaging methods. The blending functions can then

be calculated and an equation with the control points as unknown variables can be formulated for each 3D scattered point. As long as there are an equal number of scattered points and control points, this set of equations has a unique solution of control points and the surface can be calculated from this data. The shortcoming of this method is that the solution is unreliable if the matrix is close to singular.

Some research is based on the triangular approach which often handles 3D scattered points. One popular triangular method is the Matlab griddata method. It has options to allow linear, cubic, nearest neighbor and v4 (Matlab 4 griddata method) interpolations. The 'cubic' and 'v4' methods produce smooth surfaces while the 'linear' and 'nearest' have discontinuities in the first and zero'th derivatives, respectively. The ‘v4’ method produces only multiquadric surfaces. Of these options, the ‘cubic’ works best for the simple free-form surfaces. It is based on a Delaunay triangulation of the data. (http://www.mathworks.com/access/helpdesk/help/techdoc/ref/griddata.html). The Delaunay triangulation forms triangles with as few small inner angles as possible, avoiding computational errors caused by round-off when dealing with two lines with a small intersection angle. Based on the Delaunay triangulation, a triangular surface patch with a designated degree is formed within each triangle. Designated continuity between the adjacent triangular patches is satisfied during the surface reconstruction. In most applications, the cubic method is desirable since it can create a surface with C^2 continuity. Because the Delaunay triangulation is designed to maximize the minimum angle of the triangles, the

position change of one point may cause a different triangulation. Therefore, the weakness of this method is that the Delaunay triangulation is very sensitive to the distribution of the scattered points. Small changes of even one point may result in a different triangulation, and form a significantly different surface patch. Some distribution of the points may cause the interpolated surface to be wavy, which is undesirable. See Figure 4-4 (a). To avoid the wavy surface, the sampling position and distribution of the points has to be restricted. Another way to overcome the weakness of the Delaunay triangulation, while maintaining the ability to sample anywhere in the sampling area, is to uniformly sample the interpolated surface and use the griddata method again. The second surface created from the griddata method will be smooth because the triangulation will be based on a grid of points. (Figure 4-4 (b))

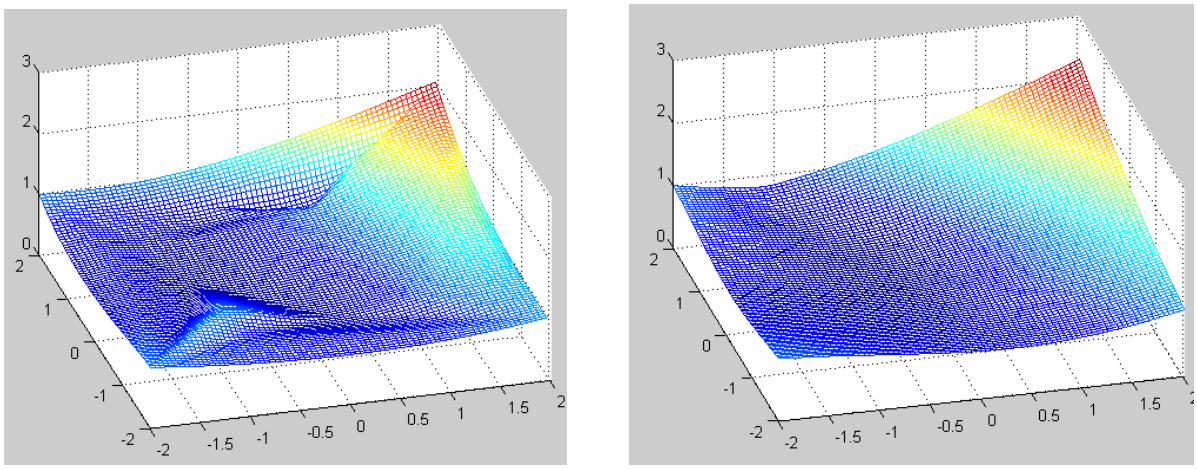

Figure 4-4 (a) Surface created with griddata method (b) Surface created from uniform sampling from (a) and using griddata again

For the uniform sampling, the sampling distance has to be decided. From the Shannon sampling theory (Shannon 1949), in order to recover the original signal, the sampling frequency should be twice the frequency of the original signal. Therefore, to reduce waviness,

the uniform sampling distance should be greater than half of the smallest wavelength allowed by the application. Although the griddata method is an interpolation method, the modified griddata method is no longer an interpolation but an approximation method, because the uniformly sampled points may not be on the part surface. Approximation is acceptable because the sampled points may not be accurate due to the measurement error. One more characteristic of the Matlab griddata method is that it can only interpolate the surface within the convex hull of the sampling points.

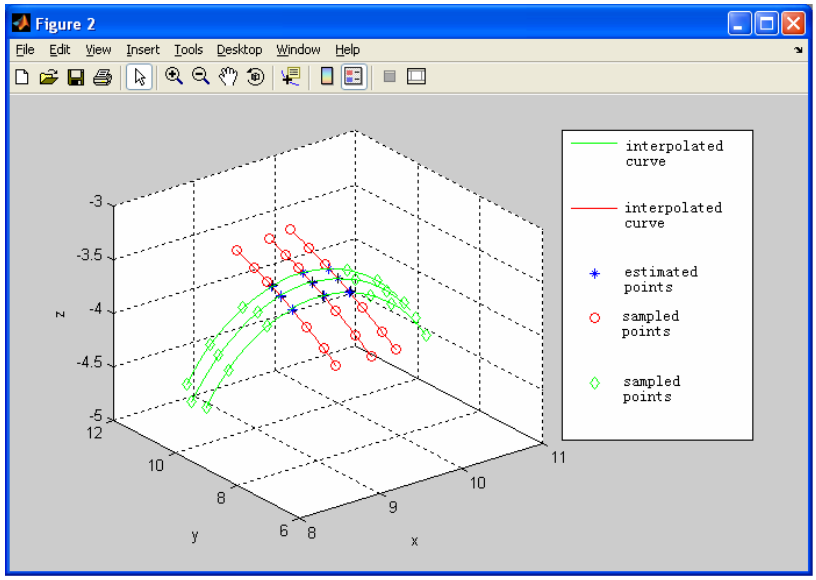

Figure 4-5 The creation of the estimated points for the modified griddata method.

For any surface reconstruction method, the challenge of minimizing the error is the lack of information in the anomaly area. In this paper, B-splines are used to estimate some points in the anomaly area. Since 2D splines are simpler than the 3D ones, points with the same x or y working coordinates are sampled for each curve. For an n^{th} degree curve, at least (n+1) points are required to achieve a good fit. As is shown in Figure 4-5, the two sets of sampled

points are selected such that the two sets of curves derived from them are orthogonal. This is done because orthogonal sets are simple. If the curves are projected to the x-y plane, the curves in the same set become parallel lines. Two orthogonal curves have one intersection when projected to the x-y plane, but they may not intersect in the 3D space. However, for a certain (x, y) coordinate, there should be only one z value for the surface, so the z value of the surface at the (x, y) coordinate is estimated as the average z values of the points on the two curves. These points are called the estimated points.

Tests were done to see how the methods and estimated points work. A 4x5 inch free-form concave surface (Figure 4-1(a)) was generated using the B-Spline surface equations so all the surface point locations were known. A 2x2 inch area near the middle of the surface was set as the anomaly area. The modified B-spline method for 3D scattered points and the Matlab "griddata" method were tested. The *error* was defined as (z'-z). Where z' is the z coordinate of a point P'(x, y, z') on the approximated surface and z is the z coordinate of a point P(x, y, z) on the original surface. Points P' and P have the same x and y coordinates. The *error band* defined in equation 4-1 is a band within which the approximated surface is different from the desired surface. Error band was used to evaluate the approximation error. The number of sampled points was used to evaluate the information needed by each method. Since the performance of the approximation methods are related to how the points are sampled, to ensure the best performance of each method, a modified two phase RMHC (Random mutation hill climbing) algorithm was used to find good heuristic

solutions from the combinations of the known surface points. For the tests with estimated points, the same estimated points were used, together with the solution from the RMHC algorithm to reconstruct the surface patch. Details of how this algorithm was applied to points sampling is stated in Appendix A. Each type of test was replicated 100 times and the results are shown in Table 4-1.

$$\text{Error band} = \begin{cases} \max(\text{error}) - \min(\text{error}), & \text{if } \max(\text{error}) \times \min(\text{error}) < 0 \\ \max(\text{abs}(\max(\text{error})), \text{abs}(\min(\text{error}))), & \text{if } \max(\text{error}) \times \min(\text{error}) >= 0 \end{cases} \quad (4\text{-}1)$$

Table 4-1 Comparison of modified Matlab "griddata" and the modified B-spline methods (EP: estimated points)

	Modified Matlab "griddata"				Modified B-Spline method			
	# of sampled points		error band (inches)		# of sampled points		error band (inches)	
	w/ EP	w/o EP	w/ EP	w/o EP	w/ EP	w/o EP	w/ EP	w/o EP
average	16+EP	16	**0.0827**	0.1443	472+EP	481	0.1657	0.2047
Standard deviation	3	3	**0.0181**	0.0246	26	33	0.0713	0.062

The test results show that the better way to approximate the surface in the anomaly area is to use the modified Matlab "griddata" method with both the sampled points and the estimated points. Tests for other concave surfaces, convex surfaces and saddle surfaces had similar results. Since the motivation of this paper is to find a simple and feasible point sampling strategy to approximate the surface beneath the anomalies, not much effort was put on finding a best surface approximation method. Since the modified Matlab griddata method works well and is simple to implement, it is chosen as the surface approximation method here. The flow chart of the modified griddata method is shown in Figure 4-6.

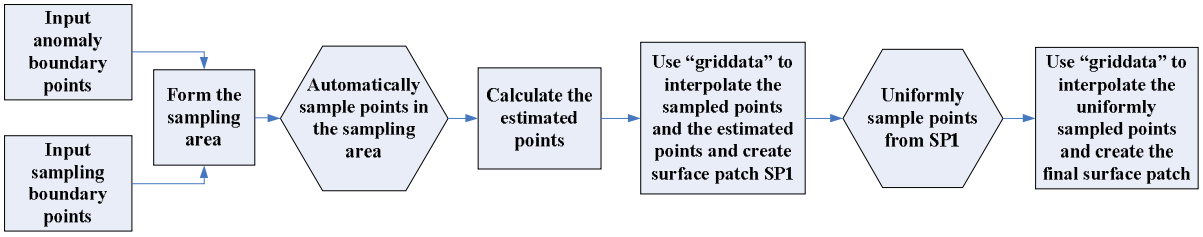

Figure 4-6 Flow chart of the modified Matlab griddata method

4.4 The Points sampling strategy

The points sampling strategy includes two main parts: 1) how many points to sample on a certain surface; 2) where to sample these points. Simulations were done to search for possible sampling patterns. The desired surface was formed by mathematical equations and simulated measurement variation of ±0.005 inches was added to the desired points when they were sampled. This value was selected based on the typical measurement error for commercial mechanical probe systems. (Geomagic 2007) The strategy will be formed from the observations of the simulation experiment results.

4.4.1 Planes

It is known that 3 points can define a plane. They should be spread away from each other to reduce the impact of measurement error. However, it is not always possible to sample them farther apart, so tests were done to find out how random sampling works. A designated number of points were sampled on the surface within a rectangular area of 5 by 4 inches, a typical dimension of the sampling area in the cleaning room grinding application. A

random measuring error within ±0.005 inches was added to each sampled data points. These data points were then used to create a plane from equation 4-2.

$$aX + bY + cZ + 1 = 0 \tag{4-2}$$

X, Y and Z were column vectors created from the x, y and z coordinates of the data points. The plane parameters were a, b and c. If there were more than 3 data points, a, b and c were parameters of a plane that was the least square approximation of all the data points.

For each created plane, the z differences of all the data points with the same x and y coordinates on the created plane and the original plane were calculated, and the maximum errors were recorded. This experiment was done 100 times for different number of sampling points to get a statistical result, which was shown in Table 4-2.

Table 4-2 Planar surface sampling results for different number of points used

# of points Sampled (sampling strategy)	Trials	Max absolute Error Mean (inches)	Standard Deviation (inches)	Max Max absolute error (inches)
3 (random sampled)	100	0.0622	0.3806	3.8197
4 (random sampled)	100	0.0137	0.0099	0.0762
5 (random sampled)	100	0.0104	0.0053	0.0383
6 (random sampled)	100	0.0098	0.0043	0.0346
3 (at least 2 inches apart from each other)	100	0.0133	0.0197	0.1997
3 (at least 2.67 inches apart from each other)	100	0.0094	0.0033	0.0188

From the results above we can see that although 3 non-collinear points can define a surface, 3 data points with error may cause great error if not sampled properly. If the 3 sampled data points were spread further from each other (1/2 and 2/3 of the shorter side of the sampling area, which were 2 and 2.67 inches respectively in the experiments), the result

is close to random sampling 4 data points. But it cannot be guaranteed that the sampling area is big enough for sampling points farther apart, so the simpler and easier way is to random sample at least 4 points on the plane.

Usually the anomaly boundary is represented by a polygon formed from a set of sampled points on the surface. These points are necessary input of the system to indicate the area that cannot be sampled. There should be at least 3 points to form the boundary polygon, so only one additional sampled point is needed if there are exactly 3 anomaly boundary points, which theoretically can be anywhere on the plane. All boundary points are sampled manually in the automatic system. It will take more points to represent the sampling boundary for the automatic system, so this additional point for approximating the plane is sampled manually. If there are more than 3 points in the anomaly boundary, no additional points need to be sampled. Sampling boundary is not required for planar surfaces.

4.4.2 Straight swept surface

A straight swept surface is constructed by sweeping a curve along a directional line. The straight swept surface can be approximated given the directional line and the section curve perpendicular to the line.

It is not hard for a human operator to tell the projection of the directional line on the x-y plane, and this information is inputted into the automatic system. To minimize the impact of the measurement error, experiments were done to test how many points will get a good fit for

a line by the least square distance method. The result shows that if only two points are sampled, they need to be farther apart. If sampled randomly, 3 points will give a much better result. To make it simple, the automatic system will choose the longest line segment in the inputted line direction in the sampling area and sample three points at both ends and at the middle. (Figure 4-7)

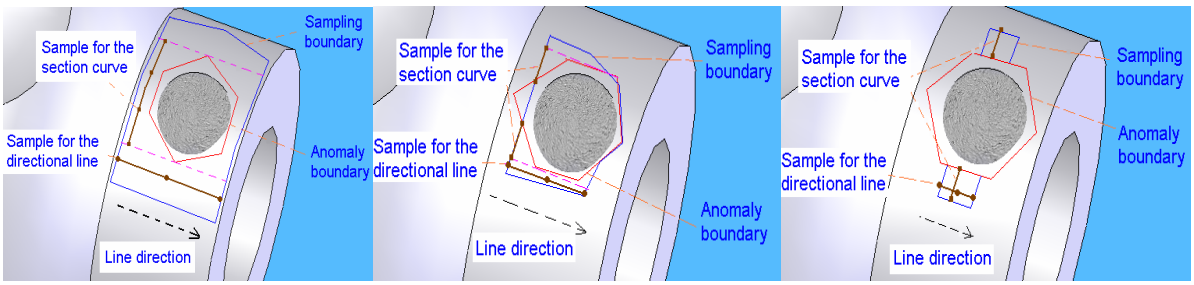

(a) **(b)** **(c)**

Figure 4-7 Different cases of points sampling for a straight swept surface (a) the entire segment of the section curve that will cross the anomaly area is available for sampling (b) part of the segment of the section curve that will cross the anomaly area is available for sampling (c) none of the segment of the section curve that will cross the anomaly area is available for sampling

When the directional line is projected to the x-y plane, the section curve is in a plane perpendicular to the projection. For a section curve with degree p, a minimum of $(p + 1)$ points are needed to reconstruct the curve. A cubic spline is used to approximate the section curve because it meets the tolerances of surface in the metalcasting industry, about 0.1 inches. The 4 points on this curve will be sampled to create a cubic curve. The section curve has to be sampled that when swept along the line, it will cross the entire anomaly area. Whenever possible, points should be sampled to get more information about the anomaly area. Because there is no information about the section curve known prior to sampling, the following

simple methods are chosen. If the entire segment of the section curve that will cross the anomaly area is available for sampling, the easiest way is to sample uniformly along this segment's projection on the x-y plane within the sampling area, See Figure 4-7(a). If no point on this segment is available for sampling, then the intersections of the longest section curve in the sampling area and the boundaries are sampled. See Figure 4-7(b). If only a portion of the segment is available for sampling, the two end points of the segment will be sampled first if possible. If an end point cannot be sampled, the closet point to the end point on the section curve outside the anomaly area is sampled. The remaining two points will be sampled to distribute points as uniformly as possible.

4.4.3 Simple Free-form surfaces

As stated in Section 4.3, all surfaces other than the planes and the straight swept surfaces are treated as free-form surfaces, and the modified Matlab "griddata" method was used for surface approximation. To use this method, when projected to the x-y plane, the entire anomaly must be in the convex hull of the sampling boundary points.

It is not easy to decide the sampling strategy for this type of surface because there is no specific information about how the surface is constructed. Therefore, a set of experiments was done to observe the number and distribution of the sampling points, and the sampling strategy was summarized from the observations of the statistical results.

4.4.3.1 The impact of the estimated points

Estimated points are used in the modified Matlab griddata method. The estimated points are created from the sampled points. The number and distribution of the estimated points directly impacts those of the sampled points, so they were studied first. As shown in Figure 4-5, the number of curves determines the number of estimated points. Tests were done on a 5 by 4 inches concave surface with a 2 by 2 inches anomaly. The points should be sampled so that the estimated points are in the anomaly area. Points for creating the curves were sampled manually so that when projected to the x-y plane, the curves divide the anomaly area into almost the same size, and the projections of the curves are parallel to either x or y axis. Points on the each curve were randomly sampled with half number of points on each side of the anomaly. The impact of different number of curves and different number of points on each curve were tested, as shown in Table 4-3.

Table 4-3 Impact of different number of estimated points

curves		Total # of points	Error band (inches)
3 curve in each set	6 points each curve	36 (sampled)+9(estimated)	0.0827
	4 points each curve	24(sampled)+9(estimated)	0.1213
2 curve in each set	6 points each curve	24(sampled)+4(estimated)	0.1597
	4 points each curve	16(sampled)+4(estimated)	0.1670

As expected, more estimated points lead to better results. More points on each curve leads to a better result and for the same number of sampled points, sampling them in the way that creates more estimated points is better. Considering the time used for sampling with a probe, 4 points on each curve is chosen.

Another set of experiments was done to see how dense the estimated points should be. The anomalies in the cleaning room application ranged from 1 inch by 1 inch to 10 inches by 10 inches. A rectangular anomaly area was used in the experiments and the length values of {1, 3.25, 5.5, 7.75, 10} inches were used for its sides. The number of sampled points is limited by the speed of the sampling probe, so less than 60 points are desired. At least 4 points are needed to approximate a cubic spline, so at most 15 curves can be used. The curves were distributed uniformly. Since saddle surfaces often need more points than the other two surface types to get a fit of close error band (see Table 4-4), only saddle surfaces were tested in the experiment. If the method works for saddle surfaces it should work for the concave and convex surfaces as well. For a certain area, the lowest number of estimated points that generated a surface satisfying the 0.1 inch surface tolerance was recorded.

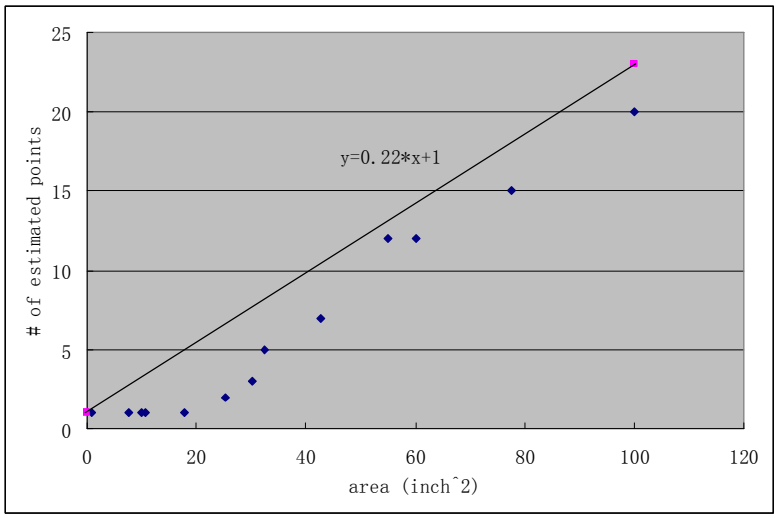

Figure 4-8 The least number of estimated points needed for a certain area

Figure 4-8 shows the average number of least estimated points needed for the saddle surfaces versus a certain area. A line with equation 4-3 was drawn to predict the number of

estimated points needed for a certain area, and to be safe, the number of estimated points predicted from the line is always higher than from the experiments. The prediction is used as the lower limit of estimated points needed for a certain area.

$$\#\text{of estimated points needed} = \lceil 0.22 * \text{area} + 1 \rceil \tag{4-3}$$

Since there is no information about the anomaly area, the simplest way is to distribute the estimated points uniformly in the anomaly area. To achieve this, the smallest rectangle whose sides are parallel to the x or y axis is formed to include the anomaly boundary points. Suppose the side lengths of the rectangle are a and b and n is the number of estimated points calculated from equation 4-3 for the area a*b. The following equations are used to calculate how many curves are needed for each set along the sides of the rectangle. The number of curves along side with length a and b is n_a, and n_b, respectively.

$$\begin{cases} \dfrac{n_a}{n_b} \approx \dfrac{a}{b} \\ n_a \times n_b \geq n \end{cases}, \ (n_a \text{ and } n_b \text{ are the smallest intergers that satisfy the equations}) \tag{4-4}$$

Solve equations 4-3 and 4-4, results in equation 4-5.

$$\begin{aligned} n_a &= \left\lceil \sqrt{0.22 \times a^2 + a \div b} \right\rceil \\ n_b &= \lceil n_a \times b \div a \rceil \end{aligned} \tag{4-5}$$

4.4.3.2 The impact of the sampling points density and distribution

To reduce the number of sampling points, points sampled to create the curves for the estimated points are also used to generate the surface. The heuristic method in Appendix A and statistical tools were used to search for the sampling points density and distribution. To

determine the pattern, sets of concave, convex and saddle surfaces were used, each with a very dense grid of surface points. To simulate the anomaly area, a rectangular area within the surface patch is designated and only those points outside the area can be the prospective sampling points. The program from the heuristic method was run 50 times for each combination of the surface patch and the anomaly size to get a mean and standard deviation of the number of sampling points and the error band. Table 4-4 shows the results for surfaces in Figure 4-1, and tests for other surface patches show similar trends.

Table 4-4 Good sampling solutions from the heuristic program

total area: 5*4 (inches)		concave		convex		saddle	
		# of points sampled	error band (inches)	# of points sampled	error band (inches)	# of points sampled	error band (inches)
anomaly 2*2 (inches)	average	16	0.0827	15	0.0758	21	0.1112
	standard deviation	3	0.0181	4	0.0193	4	0.0328
anomaly 1*1 (inches)	average	7	0.0252	7	0.0099	9	0.0178
	standard deviation	1	0.0086	1	0.0028	1	0.0064

From Table 4-4 and the results for other surface patches, it can be observed that: more points are needed for a larger anomaly area, the accuracy is decided by the size of the anomaly, and more points are needed for the saddle surface patch than the concave and convex patches.

It should be noticed that under the definition of "error band" in this paper, it is no longer true that the more sampled points there are, the better the approximated surface will be. Because the "error band" only represents the maximum deviation of the approximated surface to the original surface, deleting sampled points may not result in a larger maximum

deviation. For example, in the 5 by 4 inch sampling boundary with a 2 by 2 inch anomaly, a set of 457 points was sampled first with an error band of 0.0827 inches. Points in this set were then deleted if the deletions won't result in a larger error band. After the deletions, only 16 points in this set was left with the same error band of 0.0827 inches.

Further statistical analysis was done to study the distribution of the sampled points in the good heuristic solutions. The surface patch was projected onto the x-y plane and divided into contour strips of the same width. (Figure 4-9 (a)). For each good heuristic solution from the method in appendix A, the number of sampled points within each strip was counted and the percentage of points within the strip was calculated.

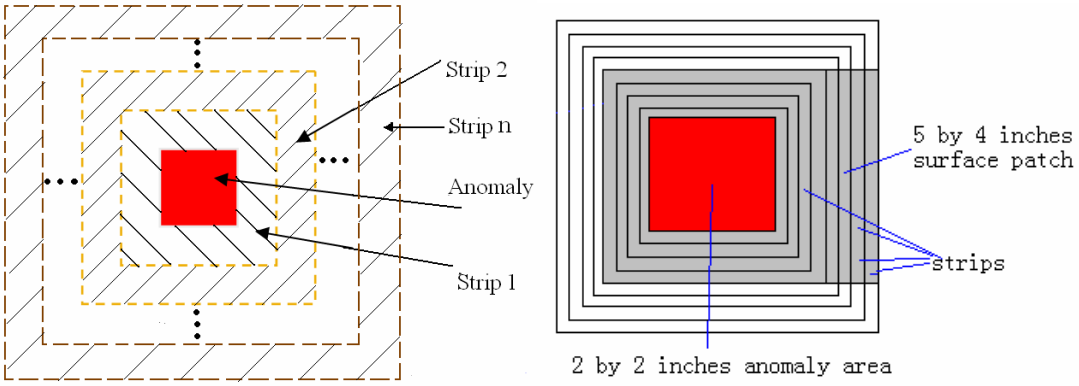

Figure 4-9 (a) Illustration of the strips used for count points distribution (b) strips on the tested surface patches (strip width 0.25 inches)

The surface patches are all 5 by 4 inches. The anomaly center is located 2 or 3 inches from the shorter side and 2 inches away from the longer sides. Therefore, some strips may partly be outside the surface patch, see Figure 4-9(b).

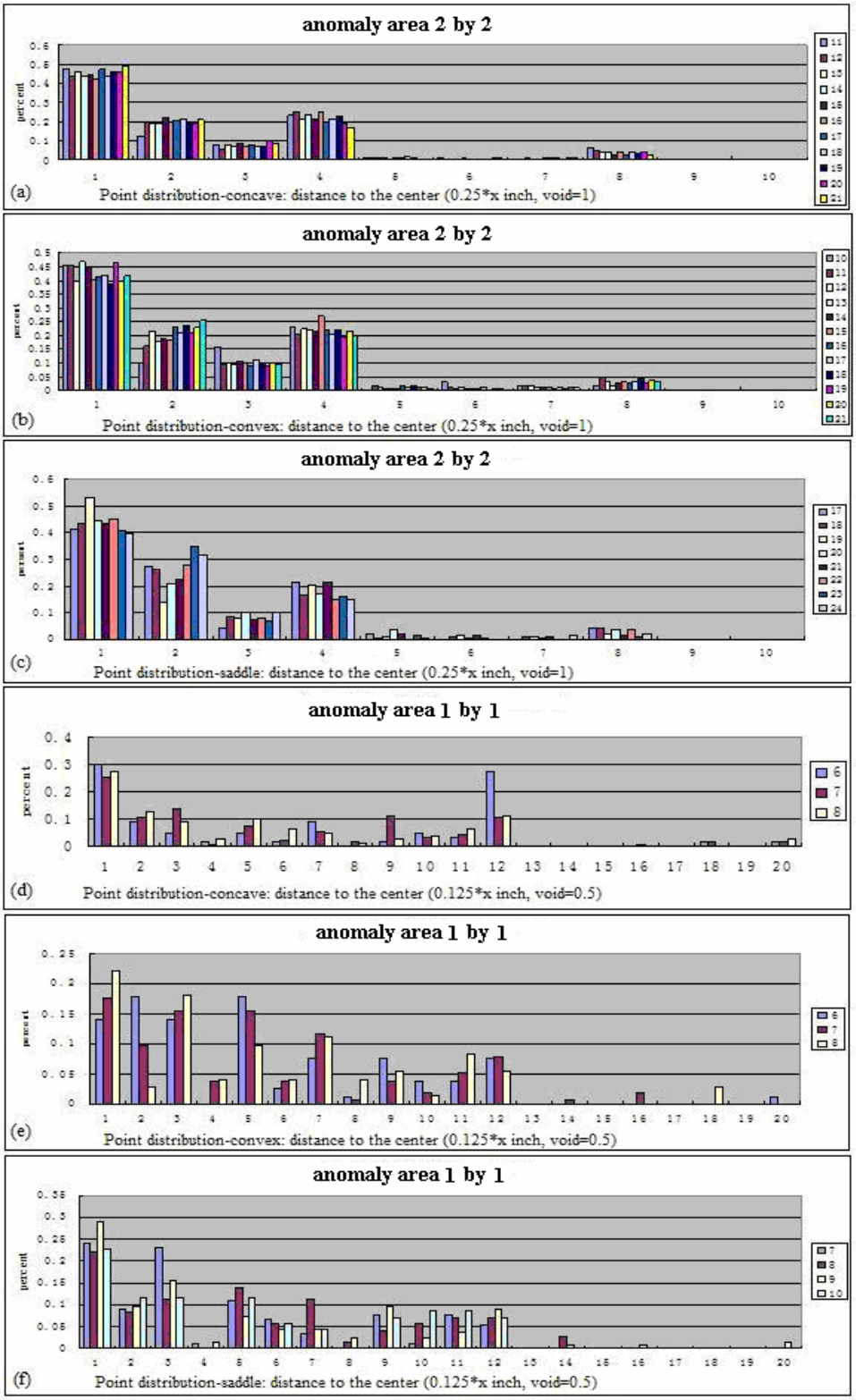

Figure 4-10 Sampling point density: percentage points in each strip vs. distance to the anomaly (legend indicates the total number of points sampled in that sampling set)

The histogram in Figure 4-10 shows the percentage of point number within each strip. The different colors represent heuristic solutions with different number of total sampled points. From Figure 4-10, it can be concluded that most sampled points are located near the anomaly boundary and the sampling boundary, and that the point density decreases as the distance to the anomaly increases.

4.4.3.3 Conclusion from the experiments

The simple sampling strategy for the simple free-form surface is described as follows:

1) Create a smallest rectangle containing the anomaly boundary. The sides of this rectangle are parallel to the x or y axes in the working coordinate system.

2) Based on the size of the rectangle, determine how many curves need to be created along each side according to equations 2 and 3. The curves are equally spaced.

3) For each curve, 4 points are sampled, two on each side of the anomaly, one of which is close to the anomaly boundary and the other close to the sampling boundary.

4.4.3.4 Testing of the strategy for the free-form surface patches

This set of sampling rules was tested on the surface patches shown in Figure 4-1. The heuristic method was run 50 times and the best solutions from the method in appendix A were compared with the simple sampling strategy in this paper. The simple strategy proposed in this paper was run 3 times with different sets of boundary points sampled by the same operator. The anomaly size and number of sampling points were varied, and the results are listed in Table 4-5. It shows that the result from the simple point sampling strategy is very close to that of the best heuristic solutions.

Table 4-5 Comparison of different sampling methods for surface approximation

		Average error band from the heuristic method (inches)	Average error band from the simple point sampling strategy (inches)
concave	2*2 anomaly, 16 points	0.0961	0.1196
	1*1 anomaly, 8 points	0.0272	0.0506
convex	2*2 anomaly, 16 points	0.0790	0.0991
	1*1 anomaly, 8 points	0.0112	0.0497
saddle	2*2 anomaly, 16 points	0.1206	0.1658
	1*1 anomaly, 8 points	0.0210	0.0615

4.4.4 Summary of the point sampling strategy for the surface types discussed in this paper

From the discussion above, the points sampling strategy is formed for an automatic point sampling and surface approximation system. First, the necessary information is inputted to the system by a human operator, and then the system will automatically decide how many sampling points are needed to approximate the surface and where to sample them.

1) Planar surfaces:

- A human operator inputs the boundary points and tells the automatic system it is a planar surface patch.
- The automatic system will check the anomaly boundary points.
- If the number of anomaly boundary points
  - >= 4, no more points will be sampled
  - else the operator will be required to sample more points on the surface
- A least square method is used to fit a plane through the anomaly boundary points and the additional points (if there is any).

2) Straight swept surfaces:

A human operator will input the following information:

- the surface type (straight swept),
- the direction of the line when projected to the x-y plane,
- the anomaly boundary points

- the sampling boundary points.

The automatic system will sample based on the above information.

Step 1: Project all points to the x-y plane. Form the anomaly polygon and the sampling polygon from the corresponding sets of projected boundary points. Calculate the sampling area, which is the sampling polygon minus the anomaly polygon.

Step 2: Search the sampling area, in the direction perpendicular to the projected line direction, for segments that can be sampled to approximate a curve that will cover the anomaly polygon when swept along the projected line direction. If the segment does not exist, ask the operator to re-sample the sampling area again, otherwise the system won't be able to sample proper points for surface patch approximation in the anomaly area.

Step 3: Sampling for the directional line. Check in the sampling boundary to find out the longest segment in the projected line direction, sample surface points with the same (x, y) coordinates as the end points and the third point anywhere on the segment in the sampling area, preferable the middle point of the segment. These points are now 3D and are used to form the line. If there are more than one segments with the same longest length, randomly choose one.

Step 4: Sampling for the section curve. Search for a segment in the sampling area that when swept along the direction line, it crosses the entire anomaly area. If such segment exists (if there are more than one of such segment, randomly choose one), find its shortest sub-segment that is still able to cross the entire anomaly area when swept along the direction line. Uniformly sample 4 points on the sub-segment. If no such segment exists, search for a combination of segments in the sampling area that when swept along the direction line, its coverage of the anomaly area is the largest. Sample the end points of the segments in the combination. If no combination exists, search for the longest segment in the sampling boundary that is perpendicular to the directional line. Sample at the end points of this segment and its intersections with the anomaly boundary.

Some examples are shown in Figure 4-11.

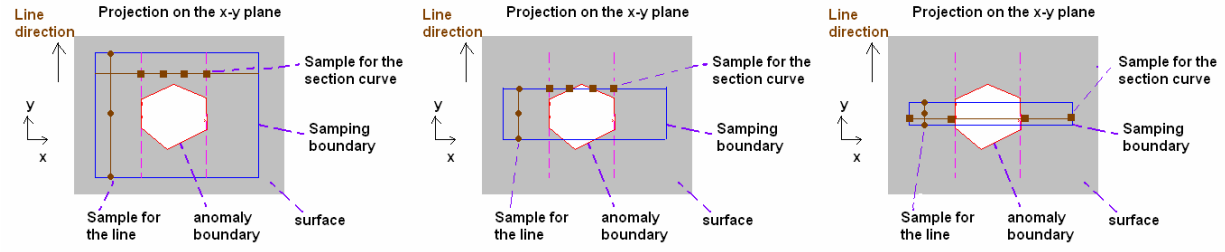

Figure 4-11 Examples of points sampling for the straight swept surface

The section curve will be approximated into a cubic spline, and all points on this curve will be shifted along the line to create the surface patch.

3) Simple Free-form surface

The human operator will input the surface type, the anomaly boundary points and the sampling boundary points.

The automatic system will do the following steps.

Step 1: Project all boundary points to the x-y plane. Form the anomaly polygon and the sampling boundary convex hull from the corresponding sets of projected boundary points. Check if the anomaly polygon is within the sampling convex hull. If not, require the operator to resample the boundary points. Calculate the sampling area, which is the sampling polygon minus the anomaly polygon.

Step 2: In the working coordinate system, find out the smallest rectangle that includes the anomaly boundary. The sides of the rectangle should be parallel to the x or y axes in the working coordinate system.

Step 3: Find out the lengths of the two perpendicular sides of the rectangle in step 2, marked as a and b, respectively (in inches). Calculate the required number of curves perpendicular to each side from equation 4-5.

Step 4: Uniformly divide the side with length a into n_a+1 segments. At each inner separation point, a line passing this point and perpendicular to this side is formed, and its intersections with the sampling area are calculated. Surface points with the same (x, y) coordinates with these intersection points are sampled. Repeat for side with length b.

An example is shown in Figure 4-12.

The automated sampled points will first be used to calculate the estimated points, and then the boundary points. The automated sampled points and the estimated points are used to approximate the surface patch by the modified Matlab griddata method.

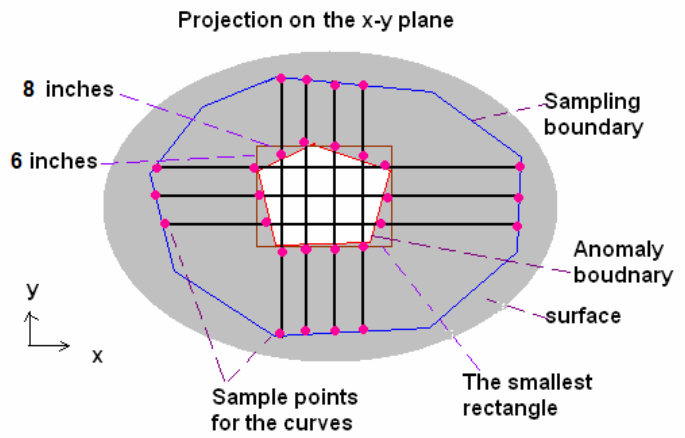

Figure 4-12 An example of point sampling for a simple free-form surface

4.5 Discussion

The approximated surfaces were compared to the desired surfaces in the experiments. The desired surfaces are not known for the applications discussed in this paper, therefore, the results from the experiments can only be used as references in these applications.

The error band defined in this paper is a band within which the approximated surface is different from the desired surface. The error band does not provide any information about the relative position of the approximated surface to the desired surface. The approximated surface can be entirely above or below the desired surface or intersect with the desired surface and still have the same error band value.

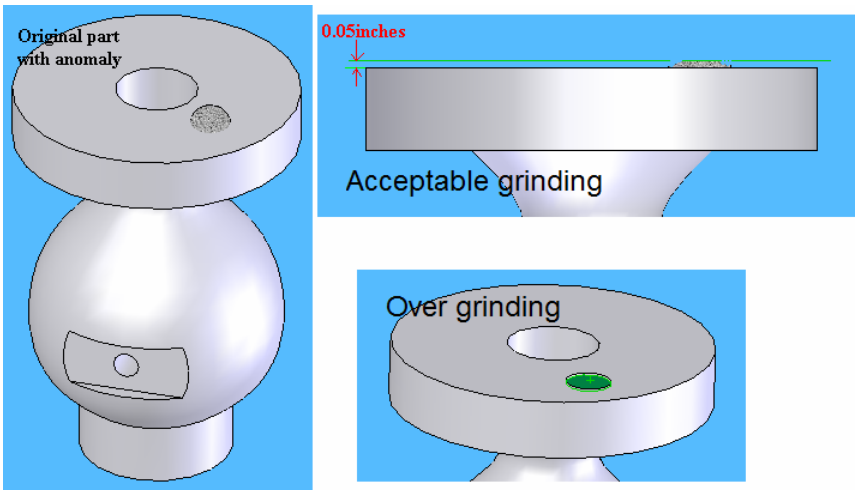

Figure 4-13 Accepted grinding and over grinding

In the cleaning room grinding application discussed in this paper overgrinding needs to be avoided. (Figure 4-13) As long as the ground surface is smooth and within the tolerance zone, a positive volume difference between the ground surface and the desired surface is acceptable. Thus, the approximated surface should be no lower (in the z-axis of the machine coordinates) than the desired surface. This can be achieved by shifting the approximated surface in the z direction for a specified distance. The "shift distance" is defined by the equations below.

$$\text{Shift distance} = \begin{cases} -\text{abs}(\min(\text{error})), \text{if} \quad \min(\text{error}) > 0 \\ \text{abs}(\min(\text{error})), \text{else} \end{cases} \tag{4-6}$$

For planar surfaces, there should be no shift distance because 3 non-linear points will define a plane. But with measurement error, the approximated plane could be under the desired plane. The worst case is that all points are sampled with the maximum negative error, so a safe shift distance would be the absolute value of the accuracy of the sampling device.

For non-planar surface patches, the shift distance will be derived from the statistical result of the negative error of the approximated surface from a set of experiments. It was observed that the length and width of the anomaly, the farthest sampling points, the surface curvature and the sampling area may all have impact on the error band and the shift distance. A factorial experiment was designed to investigate their effects. Rectangular anomalies were studied because they were simple.

In the factorial experiment, five values ([1, 3.25, 5.5, 7.75, 10] inches) were selected for the length or width of the anomaly and the farthest sampling distance. These values were selected because in the metal casting industry, most of the anomalies fall into this size range. The product of the length and the width was the area of the anomaly. The shape of the anomaly is represented by the ratio of its length to width. To test the impact of surface curvature, cylindrical surfaces were used for the straight swept surfaces, and sphere surfaces were used for the concave and convex cases with curvature changing from 1/25, 1/35, 1/45 … to 1/225, which is close to the cases in the cleaning room grinding application. For the cases that are not cylindrical in the straight swept surfaces or not spherical in the simple free-form cases, a cylindrical/spherical surface is fitted to the sampled points on the surface by the least square solution. The curvature of the fitted cylinder/sphere is called the equivalent curvature. For saddle surfaces, the equivalent curvatures were calculated in two orthogonal directions, using a cylindrical surface to approximate in each direction. For all the surfaces (other than planar), the surface variance is also calculated. It is the difference

between the sampled surface point farthest from the fitted cylinder axis or the fitted sphere center and the sampled surface point closet to the fitted cylinder axis or the fitted sphere center.

All combinations of anomaly width, anomaly length, farthest sampling distance and curvature levels were run for the cylindrical, spherical concave, spherical convex and saddle surfaces. The sampling strategy stated in this paper is used to automatically sample points on the surfaces. A normal-distribution measurement error was added into the experiments to test its impact, with mean 0 and 99% percent of the values fall into the range of [-0.005 0.005] inches, which is the average accuracy of most commercial mechanical probing systems. (GeoMagic, 2007)

Figure 4-14 are examples from the experiments showing the impacts of the factors. From all the experiments, the following were observed:

- For the same curvature, sampling area, and anomaly area, the slimmer the anomaly area, the larger the error and shift distance. (Figure 4-14 (a))
- Regardless of the anomaly size and shape, less sampling area results in a smaller error band and less shift distance. (Figure 4-14 (b))
- For the same sampling area and surface curvature, the larger the anomaly area the larger the error band and shift distance. (Figure 4-14 (c))
- Keeping other variables the same, the larger the equivalent surface curvature is, the larger the error band and shifting distance are. (Figure 4-14 (d))

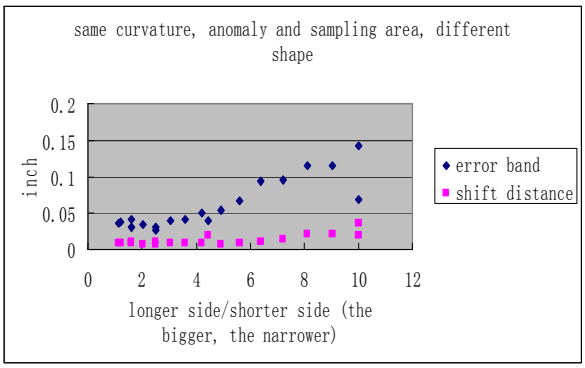

(a) impact of the anomaly shape

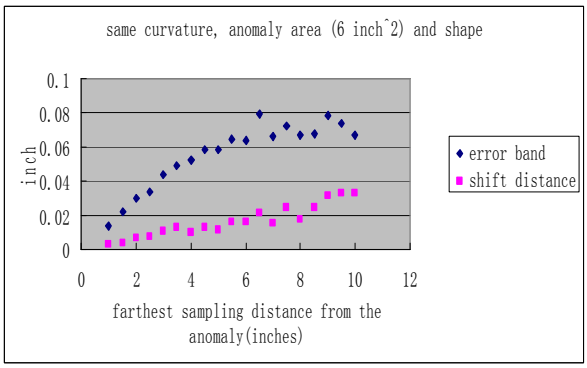

(b) impact of the sampling area

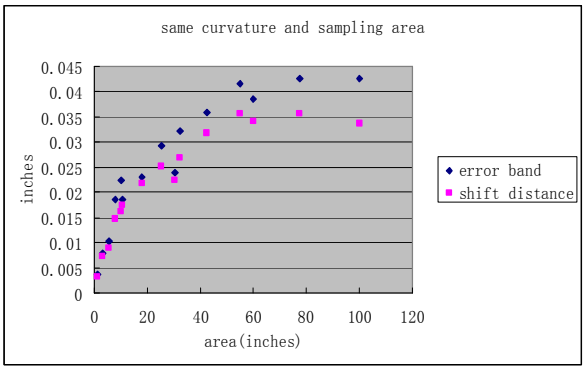

(c) impact of the anomaly area

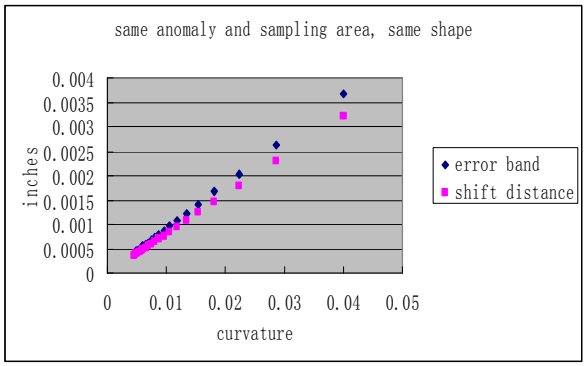

(d) impact of the curvature

Figure 4-14 Impacts of different variables on error band and shift distance

Regression methods were used to determine if an equation could be found to predict the error band and shift distance using the anomaly length, width, shape, area, equivalent surface curvature, surface variance, and farthest sampling distance. The Matlab stepwise regression method was used to reduce the number of variables. The variables with little impact on the R^2 and RMSE were eliminated, and the equivalent surface curvature, anomaly area, farthest sampling distance and surface variance were selected to form the equation used to predict the error band and shift distance for the surfaces. The equations below are the regression results from the factorial experiment data. In the factorial experiment, cylindrical surfaces were used

to represent the straight swept surfaces, and spherical surfaces were used for the simple free-form surfaces. The straight swept or simple free-form surfaces were tested with 5 surfaces that are not cylindrical or spherical and have different anomaly size. The results showed that the equations give reasonable predictions. For example, for the simple free-form convex surfaces, the average absolute difference between the prediction and actual value was 0.082 inches for the error band and 0.057 inches for the shift distance. The prediction error was higher in saddle surfaces.

Straight swept surfaces:

$$\begin{aligned}\text{error band} &= 0.2578 \times \text{equivalent curvature} + 0.0001 \times \text{anomaly area} \\ &\quad - 0.0004 \times \text{farthest sampling distance} + 0.0354 \times \text{surface variance} - 0.0004 \\ \text{shift distance} &= 0.1027 \times \text{equivalent curvature} + 0.0001 \times \text{anomaly area} \\ &\quad - 0.0005 \times \text{farthest sampling distance} + 0.0253 \times \text{surface variance} - 0.0002\end{aligned}$$

Free-form concave surfaces:

$$\begin{aligned}\text{error band} &= 0.3264 \times \text{equivalent curvature} + 0.0031 \times \text{anomaly area} \\ &\quad + 0.0013 \times \text{farthest sampling distance} + 0.0228 \times \text{surface variance} - 0.0131 \\ \text{shift distance} &= 0.2324 \times \text{equivalent curvature} + 0.0020 \times \text{anomaly area} \\ &\quad + 0.0007 \times \text{farthest sampling distance} + 0.0141 \times \text{surface variance} - 0.0096\end{aligned}$$

Free-form convex surfaces:

$$\begin{aligned}\text{error band} &= 0.3340 \times \text{equivalent curvature} + 0.0028 \times \text{anomaly area} \\ &\quad + 0.0013 \times \text{farthest sampling distance} + 0.0225 \times \text{surface variance} - 0.0127 \\ \text{shift distance} &= 0.2386 \times \text{equivalent curvature} + 0.0024 \times \text{anomaly area} \\ &\quad + 0.0007 \times \text{farthest sampling distance} + 0.0139 \times \text{surface variance} - 0.0098\end{aligned}$$

Free-form saddle surfaces:

$$\begin{aligned}\text{error band} &= 0.7953 \times \text{equivalent curvature in x direction} \\ &+ 0.1635 \times \text{equivalent curvature in y direction} \\ &+ 0.0515 \times \sqrt{\text{anomaly area}} + 0.0087 \times \text{farthest sampling distance} \\ &- 0.0417 \times \text{surface variance in x direction} \\ &- 0.0066 \times \text{surface variance in y direction} - 0.0689\end{aligned}$$

$$\begin{aligned}\text{shift distance} &= 0.2410 \times \text{equivalent curvature in x direction} \\ &+ 0.1289 \times \text{equivalent curvature in y direction} \\ &+ 0.0109 \times \sqrt{\text{anomaly area}} + 0.0040 \times \text{farthest sampling distance} \\ &- 0.0136 \times \text{surface variance in x direction} \\ &- 0.0047 \times \text{surface variance in y direction} - 0.0266\end{aligned}$$

4.6 Implementation

An automatic grinding system was designed and implemented for automatic removal of the anomalies on the castings. The sampling strategies in this paper were used to automatically sample points on the unknown surface. A novel real-time path planning strategy which was described in another paper was used to remove the anomaly. (Wang 2007)

The test parts with various anomaly shapes were designed in Solidworks and patterns of the parts with the anomalies were printed in a 3D printing rapid prototyping machine. For comparison, another set of parts without the anomalies was also made via the same method. Silicon rubber molds were made from the patterns, and used to create epoxy parts. The epoxy was chosen because it could be cut on the prototype grinding system in the laboratory. The parts without the anomalies and the parts after the automatic grinding operation were laser scanned and compared in the reverse engineering software Rapidform. Figure 4-15 shows the

CAD model of the part without anomalies, the part with anomalies, and the part after automatic grinding operation. Figure 4-16 shows the difference maps of the ground parts and the parts made without the anomalies. It can be seen that the average error is around 0.3 mm (0.012inches). The largest error in the anomaly area is less than 2.54mm (0.1 inches). While it is difficult to directly compare these results to the tolerance required by the metalcasting industry, the values seem reasonable.

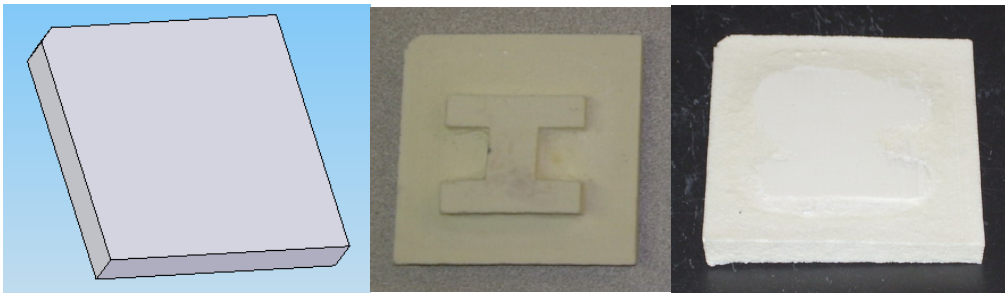

(a) part1

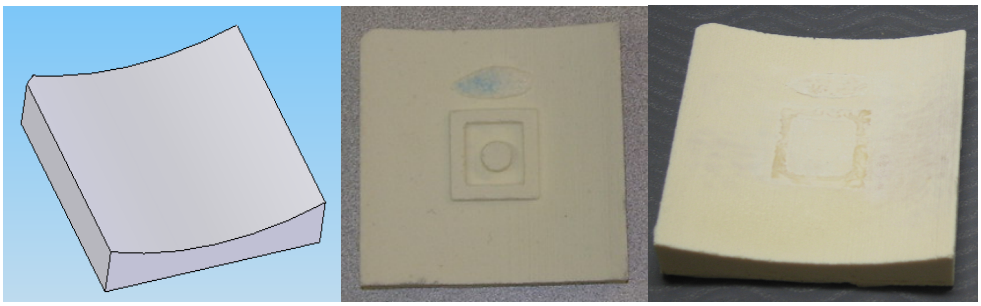

(b) part 2

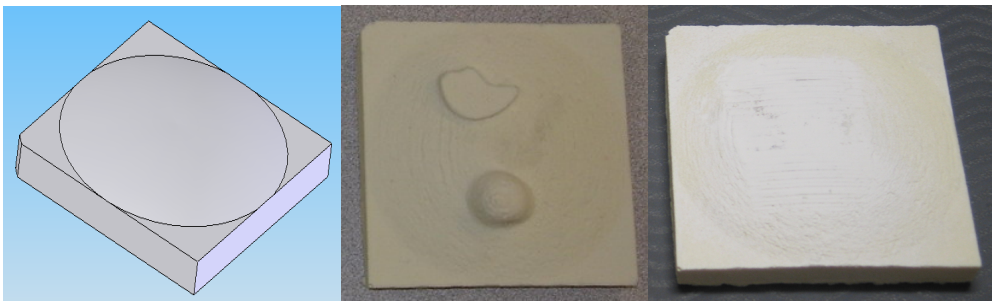

(c) part 3

Figure 4-15 The CAD model of the part without anomalies and the part before and after grinding for each of the three anomaly shapes tested

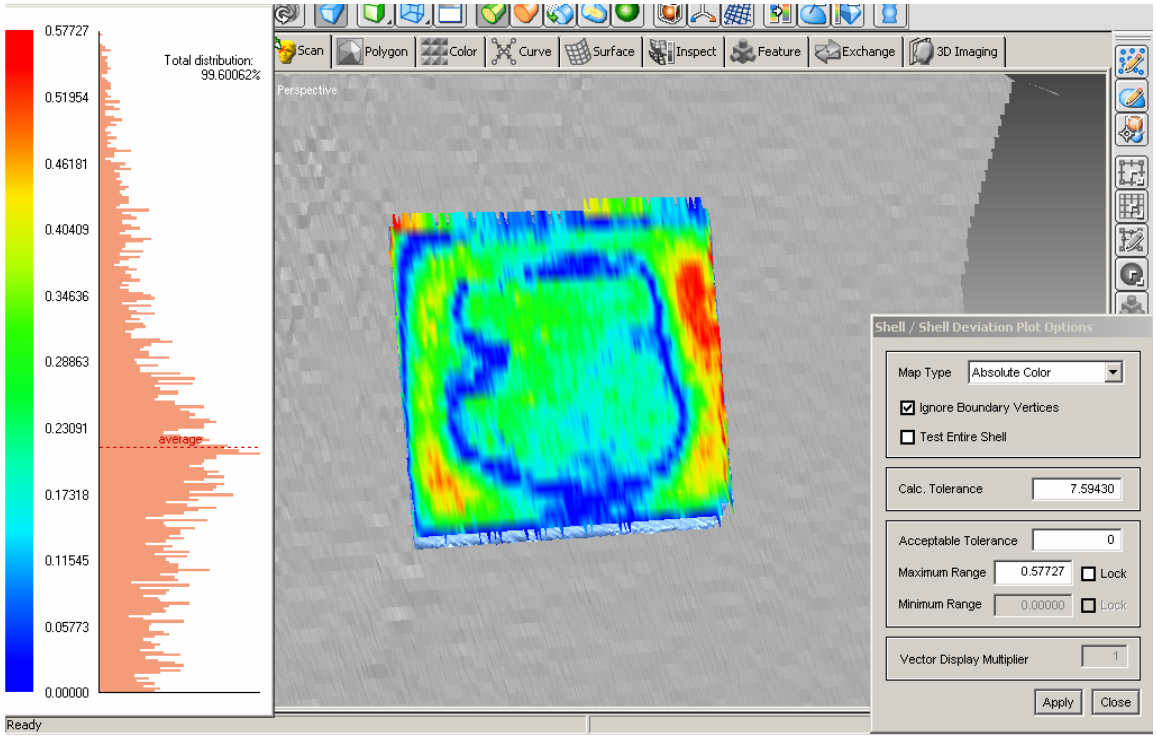

(a) part 1 (unit: mm)

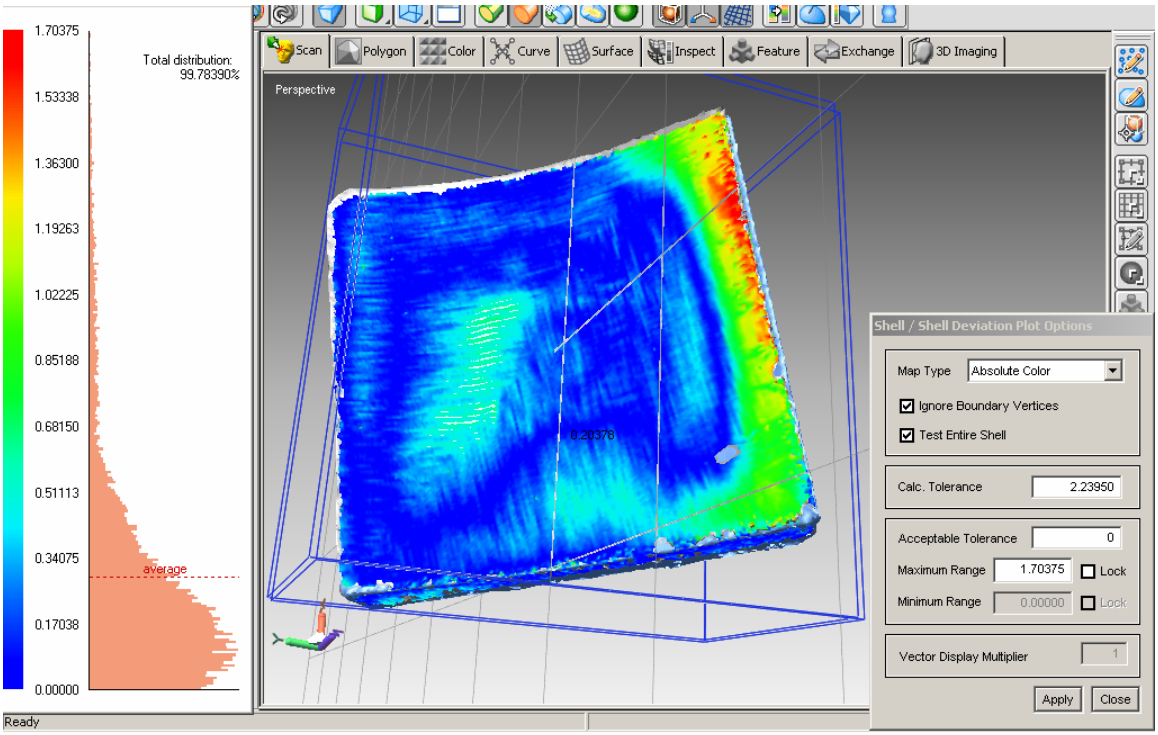

(b) part 2 (unit: mm)

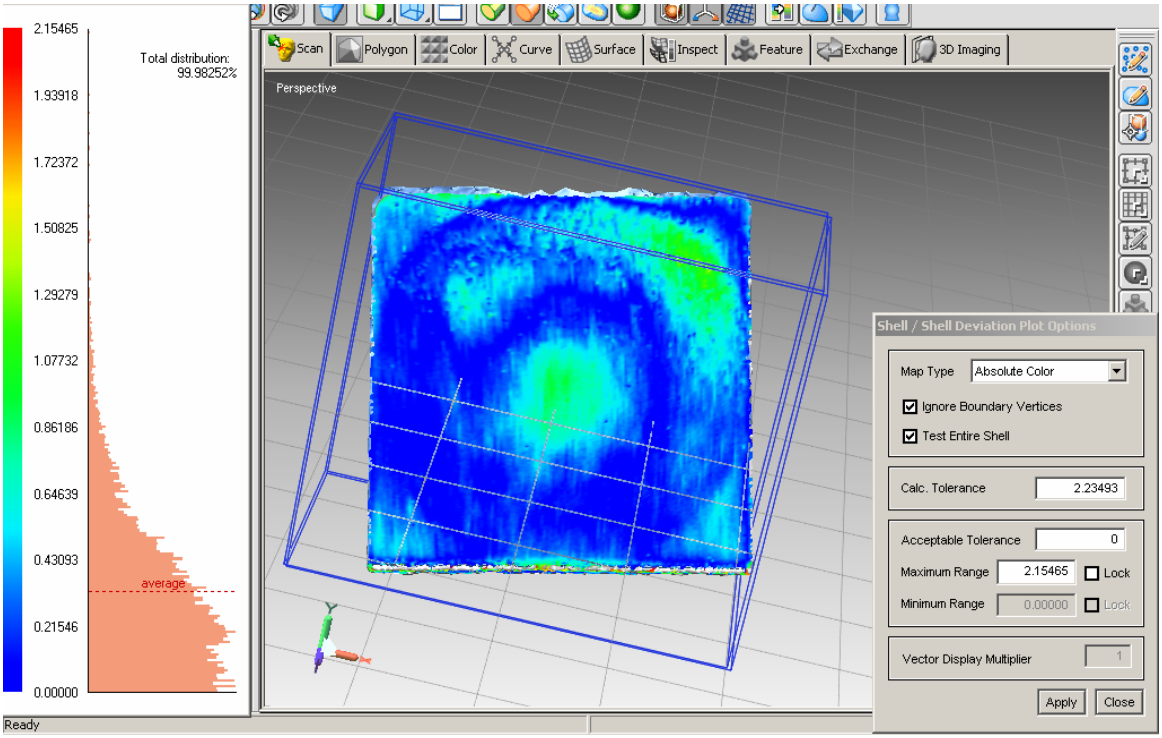

(c) part3 (unit: mm)

Figure 4-16 The difference maps of the ground parts and the parts made without the anomalies (the red regions with larger error values were not in the anomaly boundaries defined in the grinding operation)

4.7 Conclusion

This paper presented a simple and feasible point sampling strategy for reconstructing unknown surfaces. The strategies for planar surfaces, straight swept surfaces and simple free-form surfaces were concluded from the observation of designed experiments. The equations for predicting the performances of the strategies were given. The strategies were tested in an automatic grinding system and proved to meet the surface accuracy requirements of that application.

Appendix A

The optimal solution for points sampling is a combination of minimum surface points that can reconstruct a surface patch within the tolerance zone in the anomaly area. This is an instance selection problem and can be formulated as:

- Decision variable: xj=0,1 (0: instance is not chosen, 1: chosen)
- Constraints: error band < a (a: tolerance)
- Object function: minΣxj (if the constraints can be met)
  min error band(if the constraints cannot be met with any data at all)

Since there are countless combinations of the surface points, finding the optimal combination is not realistic. Heuristic methods are used to search for good enough combinations. The RMHC (Random mutation hill climbing) algorithm is able to get better heuristic solutions than generic algorithms, but it is very time consuming especially with large data sets (Mitchell 1992). Wu (2006) presented a 2-phase RMHC (Random mutation hill climbing) algorithm to achieve even better results. In this paper, a modified 2-phase RMHC (Random mutation hill climbing) algorithm is used to find some good results from the combinations of the known surface points. The modification is in the discarding step. Instances can be discarded even if this will end up with a worse result. They are discarded with a probability regarding how much worse the result is. The probability function is $p = e^{-k \cdot \max((current\_error - best\_error),0)}$ (k is selected to shape the probability function according to the specific problem). A uniformly distributed random number between 0 and 1 is generated each time a worse result of discard happens. If the random number is smaller than the probability, this instance will be discarded. Each result from the heuristic method is a set of points with their coordinates, and the error of the approximated surface from the original surface.

References

Edgeworth, Robert and Wilhelm, Robert G. (1999) "Adaptive sampling for coordinate metrology". *Precision Engineering,* 23, pp144-154

ELKOTT, DIAA F; ELMARAGHY, HODA A. and ELMARAGHY, WAGUIH H. (2002) "Automatic sampling for CMM inspection planning of free-form surfaces". *Int. j. prod. res.*, vol. 40, no. 11, pp2653-2676

Jun, Yongtae. (2005) "A piecewise hole filling algorithm in reverse engineering". *Computer-Aided Design*. 37. pp263–270

Keith, Alan R. and Prata, Aluizio Jr. (1996) "Optimum Sample Point Selection Algorithm for Interpolating Reflector Surfaces with a Prescribed Accuracy". *IEEE.* pp902-905

Lee, Seungyong; Wolberg, Geooge and Sung, YongShin. (1997) "Scattered Data Interpolation with Multilevel B-Splines". *IEEE Transactions on visualization and computer graphics*, VOL 3, NO. 3, pp228-244

Li, Y F and Liu, Z G. (2003) "Method for determining the probing points for efficient measurement and reconstruction of freeform surfaces". *MEASUREMENT SCIENCE AND TECHNOLOGY*. (v14), pp1280-1288

Mitchell, M.; Forrest, S. and Holland, J. H. (1992). "The royal road for genetic algorithms: Fitness landscapes and GA performance". *Proceedings of the First European Conference on Artificial Life*. Cambridge, MA: MIT Press. pp 245-254

Piegl, Les and Tiller, Wayne. "The NURBS Book", 2nd edition, Springer, 1997

Wang, Danni; Peters, Frank and Frank, Matthew. (2007). "A universal path planning method for material removal on surfaces with unknown anomalies". Unpublished.

Wu, Shuning. (2006) "Optimal Instance Selection for Improved Decision Trees". Priliminary proposal, pp 7-9

CHAPTER 5. A UNIVERSAL PATH PLANNING METHOD FOR MATERIAL REMOVAL ON SURFACES WITH UNKNOWN ANOMALIES

A paper to be submitted

Danni Wang[1], **Frank E. Peters** and **Matthew C. Frank**

Abstract:

In some material removal processes, the size and shape of the excess material are not known, making it very hard or inefficient for path planning using traditional methods. This paper presents an innovative universal path planning method for this type of material removal processes. Based on the desired surface of the part, the method removes the excess material layer by layer through the guidance of force feedback, until the desired surface is within the surface tolerance. The method is robust and capable of material removal without toolpath planning.

Keywords: path planning, layers, feedback, material removal, unknown anomalies

5.1 Introduction

Path planning is very important in automatic material removal processes. In most of the common material removal processes such as CNC machining, path planning is based on

[1] Primary researcher and author

known part and stock geometries, including their location and orientation. However, there are some material removal processes where this information is not known. An example is the post-shakeout material removal operations for metalcasting. Most metalcastings require some grinding after they are shaken out of the molds, done in an area commonly called the *cleaning room*. This grinding is used to remove the riser and gating contacts, possibly smooth the parting line, and correct any other surface anomalies such as burnt on sand. For castings that undergo welding in the cleaning room, grinding is used to blend these surfaces as well. Figure 5-1 illustrates examples of some surface anomalies. The locations, size and shape of the anomalies to be removed are different for each casting even if they are made from the same pattern. While the location of the riser and gating contacts are known, the orientation of the part is not. Since the stock is unknown, the typical path planning methods used in other material removal processes are not applicable.

Figure 5-1 Some example anomalies

A potential solution is to create a "virtual stock", for example, a prism that contains all the excess material, and then path can be planned based on the virtual stock and the desired geometry. This method is straightforward; however, only part of the material actually needs to be removed within this virtual stock, so this would result in a considerable inefficient

method. That is, the prismatic region would be overly large in order to fit all the shapes of the anomaly, resulting in considerable "air cutting" where the toolpaths guide tool over areas without metal.

The literature for path planning on unknown anomalies is quite limited. Most of the research on path planning has focused on designing an efficient path with minimum traveling time or distance along the surfaces. The stock and the amount of material to be removed in these previous methods are assumed to be known beforehand. (Yang 2002, Narayanaswami 2003 etc.) There are some that have focused on material removal on unknown surfaces (Jung 2004, Yin 2004, etc.), but only a very thin layer of material with the same thickness was removed. None of the previous work is truly capable of planning a path for removing unknown anomalies efficiently. Determining the real geometry of the anomalies as the stock for normal path planning method is not practicable, since the anomalies are different from one part to another, so an effective method must be able to remove material without any knowledge of the surface to be cut.

This paper presents a universal path planning method for material removal on parts with unknown anomalies. This path planning method searches through the designated area for the anomalies and a force feedback module determines the next step in real time, ensuring that every movement removes some material. This method will be able to remove all the anomalies on any part without changing the programming codes. In this paper, the

methodology is demonstrated using the problem of post-shakeout grinding in the metalcasting industry.

5.2 Assumptions and Annotations

The following assumptions are made without impacting the universality of the proposed path planning method.

1) The desired surface after grinding is either given from the CAD model or approximated from reverse engineering areas near the anomaly.

2) The desired surface has been transformed into the machine coordinate system.

3) A boundary polygon is given that contains the anomalies that need to be removed, indicating the working area on the surfaces. It doesn't specify the exact locations of each anomaly, but gives an area within which the path planning method will be searching for the anomalies. If no polygon is specified then the boundary of the CAD model or the approximated surface can be used.

4) The cutting force is allowed to change in a range within a minimum and a maximum value. The maximum force is an empirical value under which the tool can safely and effiently work. The minimum force is also an empirical value. When keeping other factors the same, the depth of cut is proportional to the cutting force. A relatively high average force is desired to ensure efficient cutting. Therefore, the closer the minimum force is to the maximum force, the higher the average force.

5) The anomalies are usually thicker than the maximum depth of cut.

For the work in this paper, a zig-zag (stair case) pattern is utilized. While other patterns may be more efficient, this is not the focus of this paper. However, the techniques developed would be applicable to most other cutting patterns.

Listed below are annotations used in this paper.

F_{max}: maximum cutting force, constant for each tool and part material combination

F_{min}: minimum cutting force, constant for each tool and part material combination
F_{down}: the cutting force which will signal for the system to move down to the next layer
F_c: the current cutting force, a real time variable
Pass: a pass is a straight line segment (or a stair) in the stair case tool path (From point C to point D in Figure 5-2)
Cut: a cut is a series of continuous passes with the same step over direction (From point A to point B in Figure 5-2)
F_a: the maximum cutting force within a cut

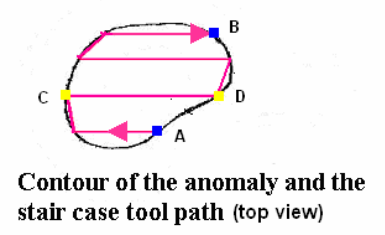

Figure 5-2 Anomaly contour and cutting paths

5.3 A Layer-based Real-time Path Planning Strategy

The greatest challenge in planning the path for removing unknown anomalies on the surfaces is the lack of information about the anomaly's location, size and shape. Methods such as creep feed grinding cannot be directly applied because of the dangerous cutting force when plunging into a thick anomaly. A method is needed to search through the working region and guide the tool to only work on the anomalies efficiently and effectively.

To accommodate this type of grinding, a compliance mechanism was incorporated that is attached to the tool to prevent potential tool damage caused by a large cutting force, and to increase cutting efficiency. A simple design that satisfies this assumption is shown in Figure 5-3. The spring is acting as the compliance device. When the grinding wheel plunges into something thick, the spring will be compressed and the grinder is raised to reduce the force. Another option is a rigid system with a force sensor, but the system may not be quick enough

to respond to a high force condition. The spring is also used to generate the cutting force against the part. The deformation of the spring can keep the grinder working on the anomaly most of the time.

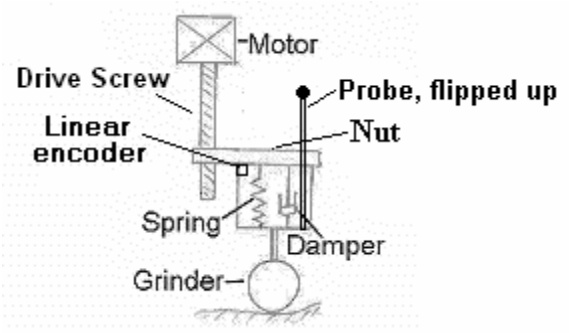

Figure 5-3 A design example of the compliance mechanism

5.3.1 Layers

Since the anomaly thickness is often larger than the maximum depth of cut, multiple iterations will be needed to remove the anomalies, and the tool has to be positioned to reference surfaces at different heights to remove the anomalies from top to bottom. Therefore, a layer concept is introduced to divide the anomalies into tiers with appropriate thickness. The layer-based path planning method will guide the tool to remove the anomalies in each layer and switch between the layers (up or down) if the current grinding force is not appropriate.

The desired surface is the lower boundary of layer 1. The boundaries of the other layers are created by shifting the desired surface along the Z axis. (Figure 5-4) The lower boundary of each layer is used as the reference surface for that layer and the tool will attempt to create

the reference surface in each layer. There are two important parameters for the layers: layer thickness and the distance between the lower boundaries of the adjacent layers.

The layer thickness should be defined that when the cutting force is maintained within the force range, the tool is working in this layer. Therefore, layer thickness is decided by the working force range. According to the Hooke's law, it is defined in equation 5-1.

$$\text{layer thickness} = (F_{max} - F_{min})/k \tag{5-1}$$

$$(\text{lower boundary of layer } n+1) - (\text{lower boundary of layer } n) = (F_{max} - F_{down})/k \tag{5-2}$$

where k is the spring constant.

Equation 5-2 defines the distance between the lower boundaries of the adjacent layers. The depth of cut is usually less than the layer thickness. During the first cut in a layer, the depth of cut is larger since a thicker excess material compresses the wheel more and results in a larger grinding force. As more cuts are taken in a layer, the depth of cut lessens, reducing the average material removal rate in this layer. Therefore, F_{down} and the concept of "overlapping layers" are introduced to increase the average material removal rate. F_{down} is an experiential value between F_{min} and F_{max}. When the maximum force in a cut (which is defined as F_a) is less than F_{down}, the tool will move down a layer (i.e. the reference surface will become the next one below). When this happens, the excess material in layer n+1 hasn't all been removed yet. Equation 5-2 ensures that the remained material in layer n+1 is also in layer n and will be removed in layer n. Since the reference surface has changed to the reference surface in a lower layer, the spring will be compressed more, generating a larger

cutting force. As a consequence, more material will be removed given other conditions (feed rate, etc.) remaining the same.

There are three cases of overlapping layers with different relations among F_{max}, F_{min} and F_{down}. Each case has its pros and cons. The case that should be used in the application is decided by the anomalies.

Case 1: $F_{down} > (F_{min} + F_{max}) / 2$

The layers in this case are illustrated in Figure 5-4(a). Once the largest force in a cut (F_a) is smaller than F_{down}, the tool is moved down a layer, and the reference surface is lower, which causes the spring to compress more, producing a higher force. A larger F_{down} forces the tool to go down earlier to increase the working force. This is more efficient since a higher force results in a larger depth of cut and a higher material removal rate. But in this case, there is more overlap of the layers, which results in more layers for the same anomaly height.

Case 2: $F_{down} < (F_{min} + F_{max}) / 2$

The layers in this case are illustrated in Figure 5-4(b). Since F_{down} is the smallest in this case, the tool will spend more time working in a higher layer before moving down. It is the least efficient case. However, it yields the fewest number of layers for a given anomaly height.

Case 3: $F_{down} = (F_{min} + F_{max}) / 2$

The simplest case is where we simply set the F_{down} to the average of the minimum and maximum cutting force (Figure 5-4(c)). In this case, the number of layers is no more than case 1 and no less than case 2.

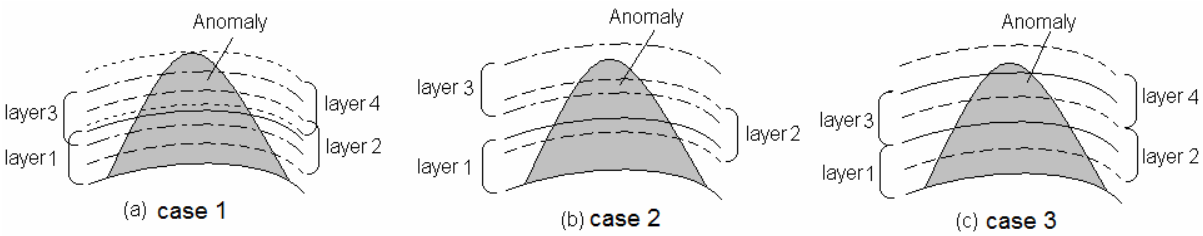

Figure 5-4 Three cases of the overlapping layers (Side view) (a) $F_{down} > (F_{min} + F_{max}) / 2$, more efficient, more layers (b) $F_{down} < (F_{min} + F_{max}) / 2$, less efficient, less layers (c) $F_{down} = (F_{min} + F_{max}) / 2$, performance and number of layers are between (a) and (b)

Although a higher average cutting force is often preferred, the larger number of layers may cause some problem when the tool plunges into a thick anomaly with a steep increase at the edge. As the algorithm is designed to be raised one layer at a time, for the cases with a higher average force, it takes more time for the tool to be moved up to a position where the cutting force is within the desired range, increasing the possibility of system damage under excessive cutting force. So the case that should be used depends on what the majority of the anomalies might be like in any specific application. If this cannot be determined, then the safest method is to use case 3.

5.3.2 The Path Planning Strategy

Cutting starts from an initial point on the anomaly boundary. The feed direction is inputted by the operator. If the feed direction is along the y axis and the step over along the x axis, the initial point will be the point with the smallest y coordinate within the points with

the same smallest x coordinate. (Figure 5-5(a)) If the feed direction is along the x axis and the step over along the y axis, the initial point will be the point with the smallest x coordinate within the points with the same smallest y coordinate. (Figure 5-5(b)) The initial point is on the anomaly boundary which is on the good surface. Since the initial point is on the part surface, it is in layer 1.

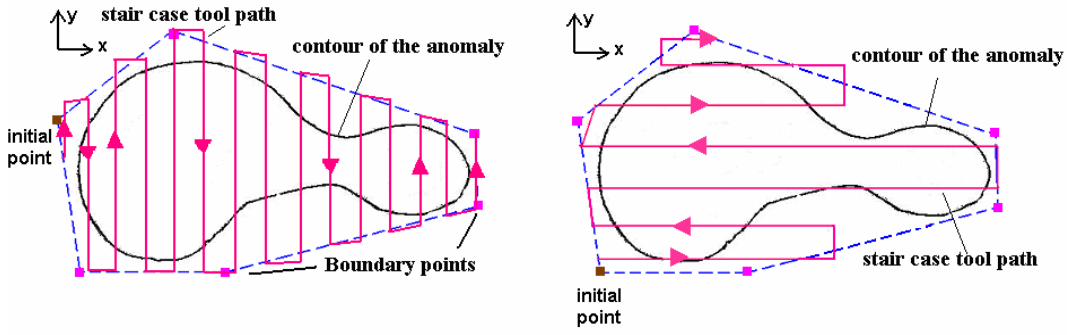

(a) feed along y axis (b) feed along x axis

Figure 5-5 Selection of initial point and corresponding zig-zag path

Initially the system will attempt to position the tool to create the desired surface. The cutting force is monitored in real time, and the next movement is determined based on the following conditions.

1) If the cutting force exceeds the maximum, the tool will be moved up to a layer in which the force is within the desired range;

2) If the current layer is layer 1, the tool will canvas the entire anomaly area with the stair case tool path as long as the force is smaller than the maximum. When the tool path is finished in layer 1, it will check whether the surface tolerance is met. If yes, then cutting of the part is finished; if not, it will go to the initial point and start the stair case tool path in layer 1 again. The cutting in layer 1 could be interrupted if the current cutting force exceeds the maximum.

3) If the current layer is higher than layer 1:
   a) When the force is in the desired range, the tool will follow the zig-zag pattern in the current layer to remove the excess material in the anomaly boundary;

b) In a pass, when the current cutting force drops below the minimum force, it indicates the end of a pass, so the tool should step over (move to the next stair) and continue the zig-zag pattern;

c) If the current cutting force is smaller than the minimum at the beginning of a pass, it indicates the end of a cut. (Point C in Figure 5-6) If the F_a in this cut is larger than F_{down}, the tool will be moved to the position when it was raised to this layer (point A in Figure 5-6) and start the zig-zag pattern in the current layer again; if F_a is smaller than F_{down}, the tool will be moved down one layer to the point before it was raised (point A' in Figure 5-6) and continue the path it was on.

Layer 1 is the only layer that the tool must cross the entire area within the boundary. For the other layers, the strategy will ensure that the tool is working on the anomalies most of the time, and does not have to cover the entire anomaly boundary. (Figure 5-6) The stair case tool path is created in real time in the different layers.

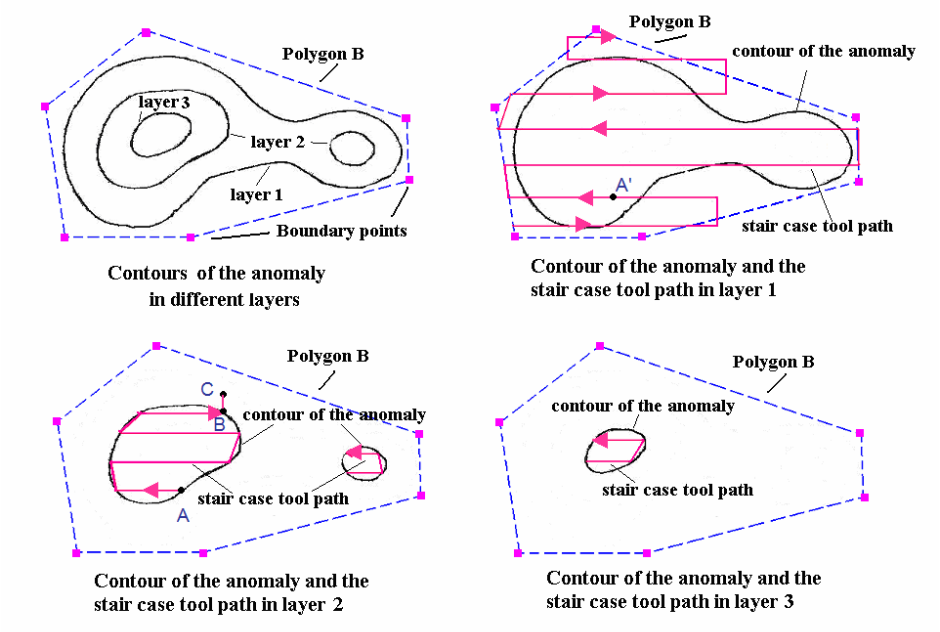

Figure 5-6 Tool Paths in Different Layers (Top View, path in the figure may be interrupted and moved to an upper layer when the working force exceeds maximum)

This is a real-time path planning method, which generates the next step based on the position and force feedback during machining. The location of the next point is calculated based on the equations below.

Reference surfaces:

$$S_{Lk} = f_{shift}\,(S_{desire},\ (L_k\text{-}1)*(F_{max}\text{-}F_{down})/k), \tag{5-3}$$

Initial point:

$n = 1$,

$L_k=1$,

$$x_1 = \min\,(x_{B1}, x_{B2}, \ldots), \tag{5-4}$$

$$y_1 = \min\,(y_{Bi} \mid x_{Bi} = x_1), \tag{5-5}$$

$$z_1 = f_z\,(x_1,\ y_1,\ L,\ S_L) \tag{5-6}$$

For any n=k (k>1),

$$(x_k, y_k, L_k) = f_{stair}\,(x_{k-1}, y_{k-1}, F_{k-1}, \{B_1, B_2\ldots\}), \tag{5-7}$$

$$z_k = f_z\,(x_k, y_k, L_k, S_{Lk}) \tag{5-8}$$

Where:

S_{desire} is the desired surface;

f_{shift} is the function used to shift the surfaces, which keeps the x and y coordinates the same while shifting the z coordinates;

L_k is the current layer number;

S_{Lk} is the reference surface in layer L_k;

$\{B_1, B_2\ldots\}$ is the set of boundary points;

x_{Bi}, y_{Bi} are the x, y value of the boundary point B_i;

$f_z(x, y, L, S_{Lk})$ is the function that searches for the z value of the point(x, y) in known surface S_{Lk};

n is the n^{th} point from start;

(x_n, y_n, z_n) is the n^{th} point's x-y-z location;

L_n and F_n are the layer and force at the n^{th} step;

f_{stair} indicates a stair case tool path to find the next x-y location.

The (x, y, z) coordinates given from the above equations are the coordinates of the contact points. The dimension of the tool and the approximated surface normal should be taken into account when calculating the tool path. This is similar to the tool compensation in CNC machining, so it is adopted here and not stated further in this paper.

For grinding operations, the wheel will wear over time causing a diameter change, so the system needs to be occasionally recalibrated. A calibration point $P_0(x_0, y_0, z_0)$ is set on a flat hard plate fixed to the system assembly and used to calibrate the grinding wheel. Before and during the grinding operation, the grinding wheel must touch off from this point in order to measure the diameter of the wheel. The system will track the grinding time for each wheel and calibrate the wheel diameter periodically based on operating time and variables such as wheel type, cutting force, and casting material.

The path planning process flow is illustrated in Figure 5-7.

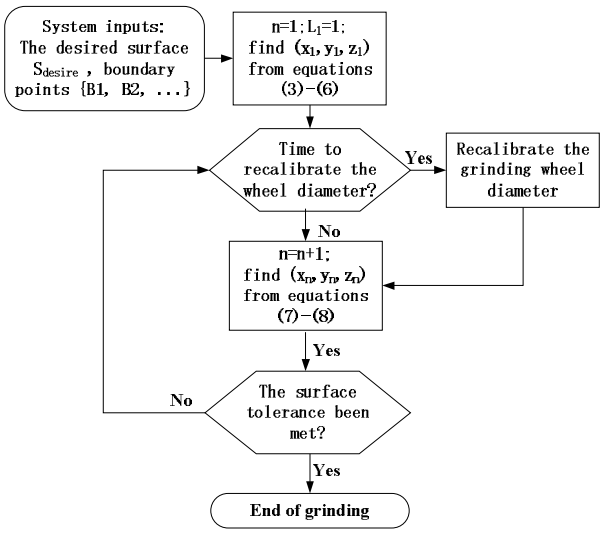

Figure 5-7 Real-time Path Planning Flow Chart

5.3.3 Examples

Figure 5-8 illustrates how the anomalies on a surface are removed step by step following the path planning strategy proposed in this paper.

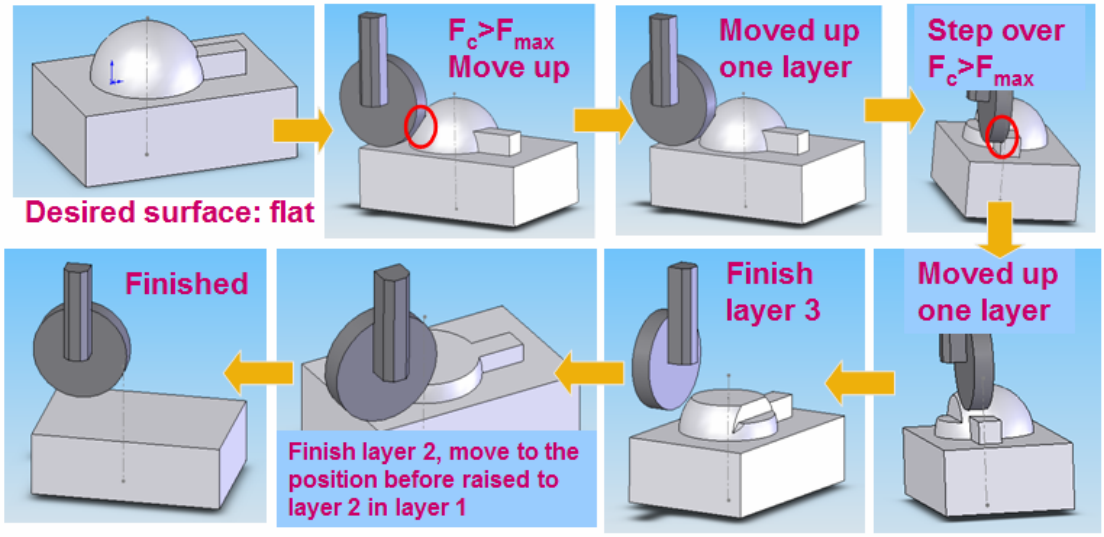

(a) removal of an anomaly with three layers

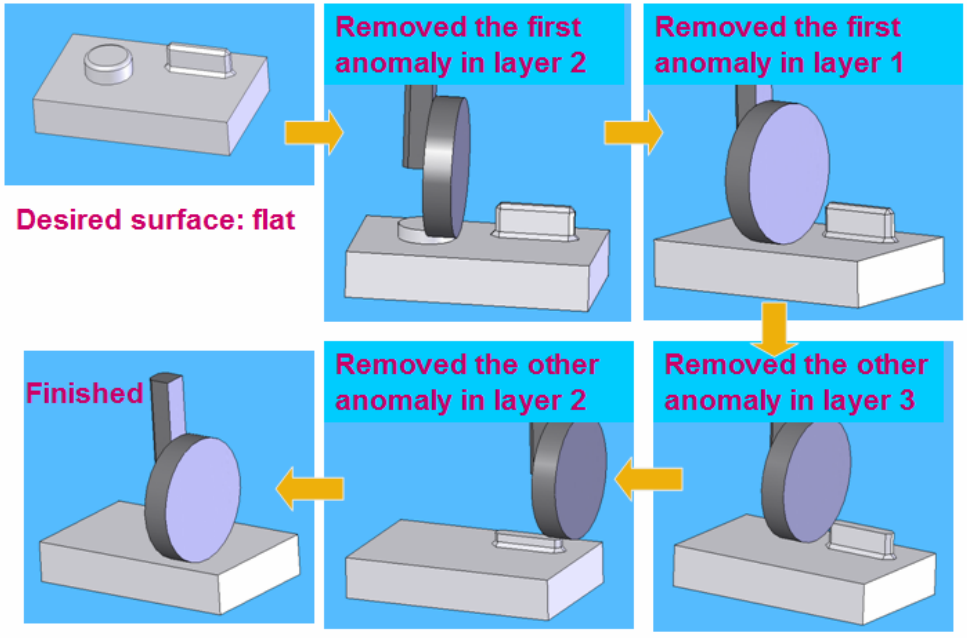

(b) removal of two anomalies in the same boundary

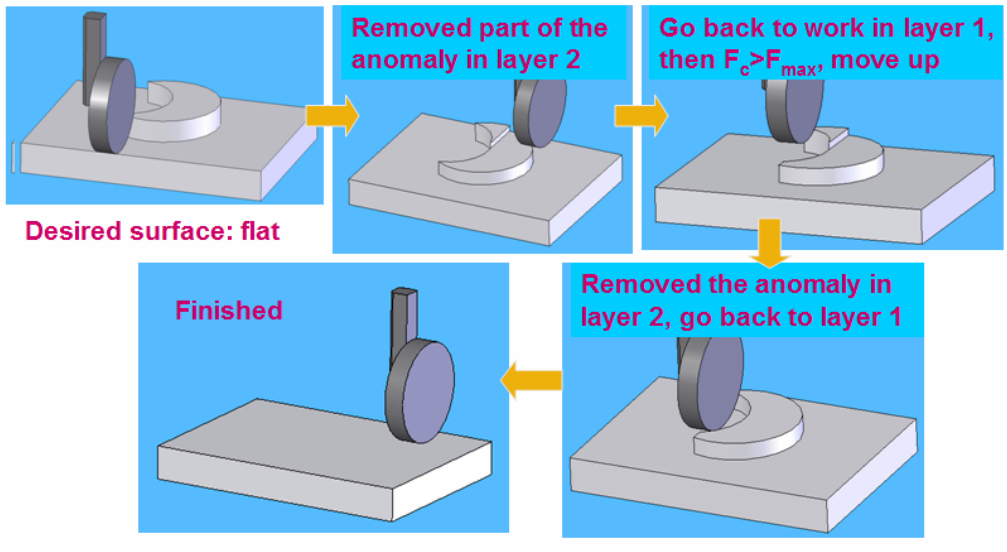

(c) removal of a moon shaped anomaly

Figure 5-8 Examples of the removal of the anomalies

5.4 Simulation and implementation

A simulation was conducted to test the path planning strategy. A surface scanned from the bottom of a casting was used as the working surface with an anomaly. Points were sampled from the surface to approximate the desired surface. The boundary points indicating the working region were also given. (Figure 5-9) The different colors represent different Z height of the surface.

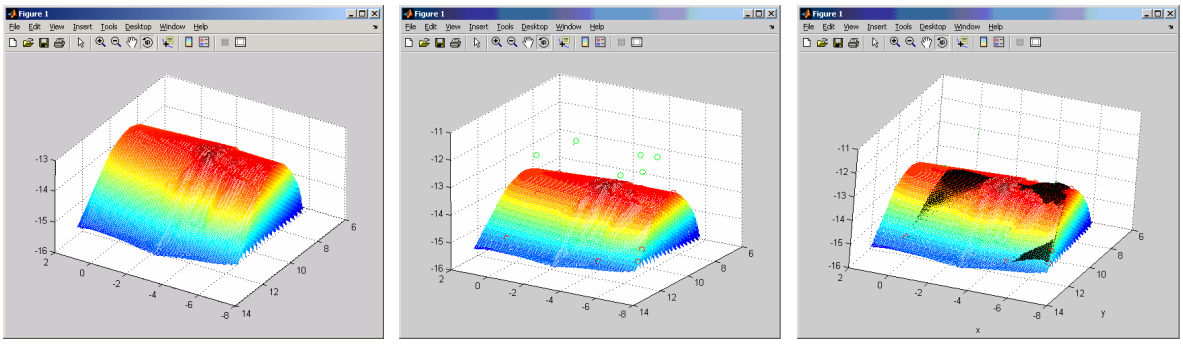

(a) (b) (c)

Figure 5-9 (a) The scanned original surface; (b) The original surface with the reference points (circles on the surface, red) and boundary points projected to a plane parallel to the x-y plane(circles above the surface, green); (c) The approximated surface patch. (represented by the darkest (black) dots)

Some parameters such as the *k* and maximum and minimum force used to decide layer depth were chosen from small experiments in foundries and based on operator observations. Figure 5-10 shows the surface after simulated grinding. By comparing with the anomaly boundary points, it can be seen that the anomaly in the boundary was removed and the remaining anomaly was not in the defined anomaly boundary. The result illustrates that the path planning method can remove the anomaly as expected.

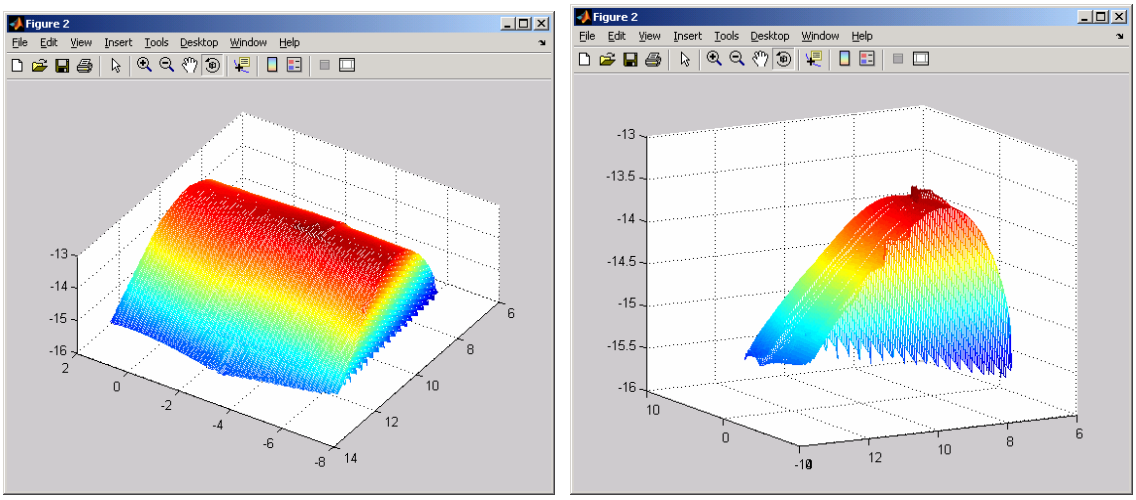

Figure 5-10 different viewing angles of the surface after simulated grinding

An automatic grinding system was designed and implemented for automatic removal the anomalies on castings. A simple point sampling strategy (Wang 2007) was used to automatically sample points on the unknown surface and the approximated surface was created from these points. The real-time path planning strategy in this paper was used to remove the anomaly.

The test parts were designed in Solidworks with different shapes of anomalies. Patterns of the parts with the anomalies were printed in a 3D rapid prototyping machine. Silicon rubber molds were made from the patterns from which epoxy parts were made. The epoxy was chosen to illustrate material removal using grinding in the prototype system. To provide a baseline, another set of parts without the anomalies were also printed in the 3D rapid prototyping machine. The parts without the anomalies and the parts after the automatic grinding operation were laser scanned and compared in the reverse engineering software Rapidform. Figure 5-11 shows the CAD model of the part as well as the part before and after the automatic grinding operation. Figure 5-12 shows the difference maps of the finished part with respect to the part made without the anomalies. It can be seen that the average error is around 0.3 mm (0.012inches). This is a reasonable number compared to the tolerances that are required of the full scale process if implemented in grinding steel, and the surface approximation error from the points sampling strategy is the main error source. The area with the largest error is actually not in the anomaly area, and is extraneous error from the pattern

and molding making steps. The test result shows that the layer-base path planning algorithm works effectively as expected.

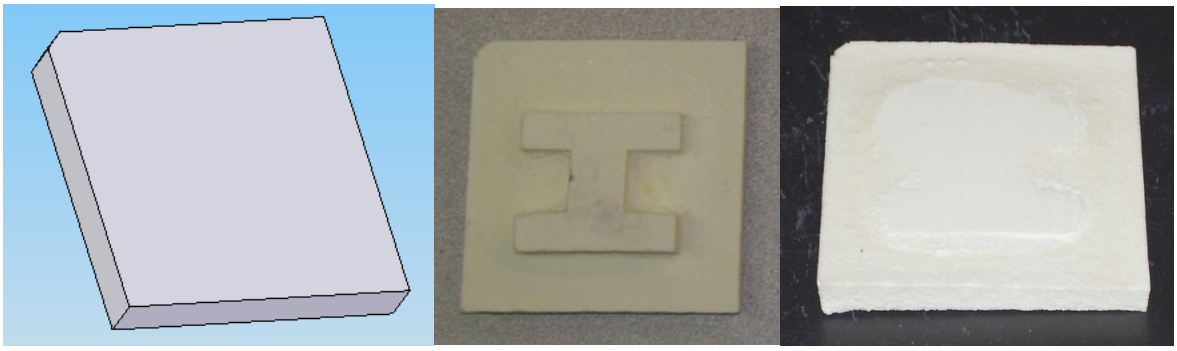

(a) part1

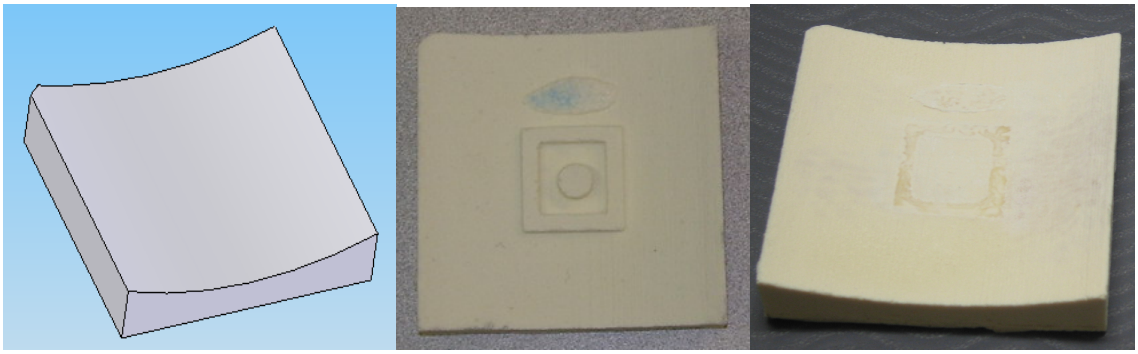

(b) part 2

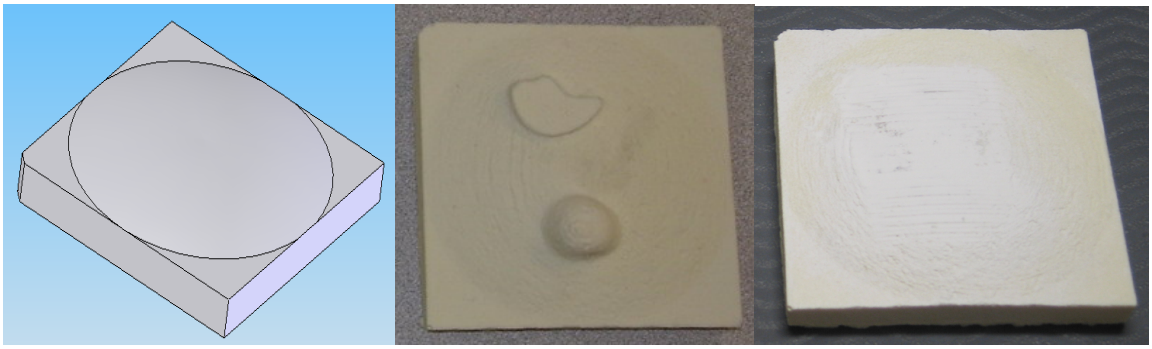

(c) part 3

Figure 5-11 the CAD model of the parts w/o anomalies and the parts before and after grinding for each of the three anomaly shapes tested

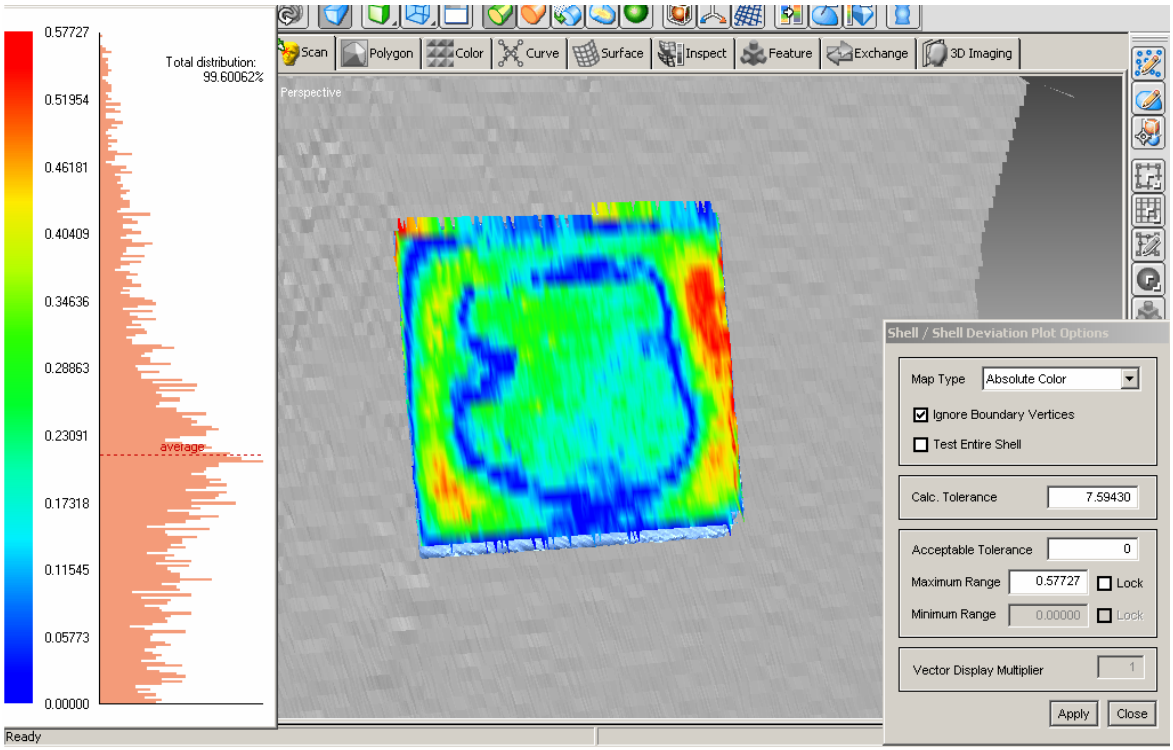

(a) part 1 (unit: mm)

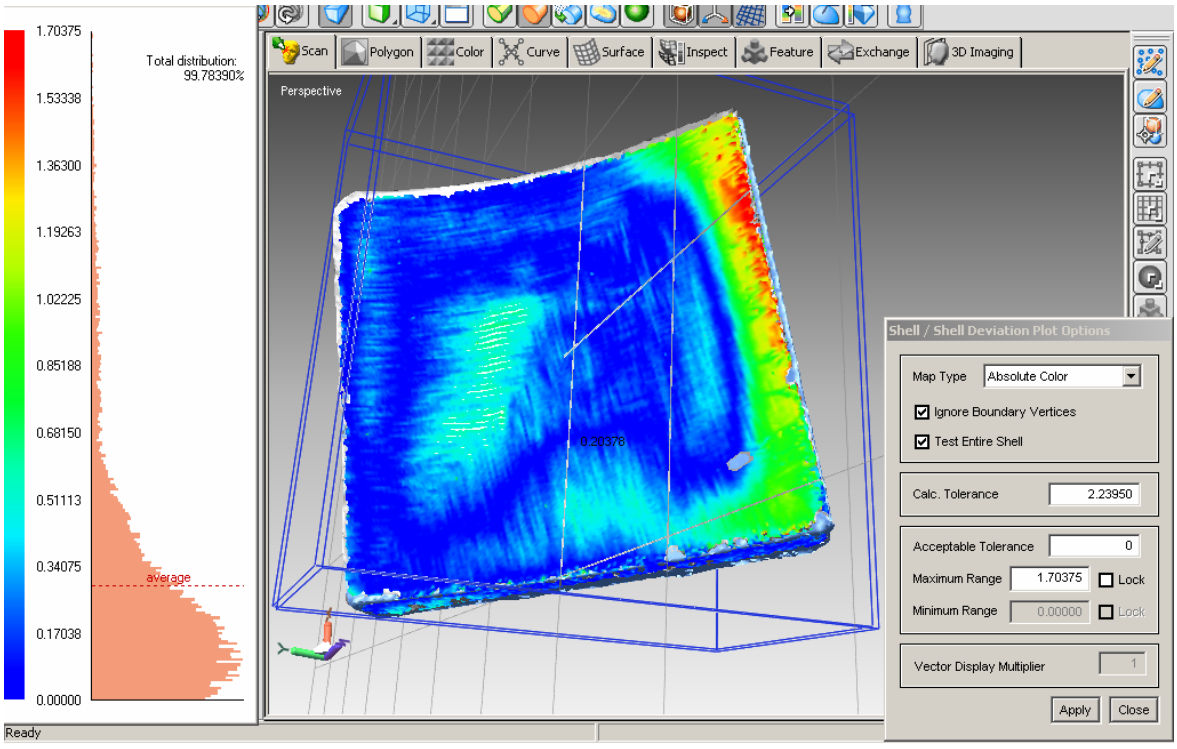

(b) part 2 (unit: mm)

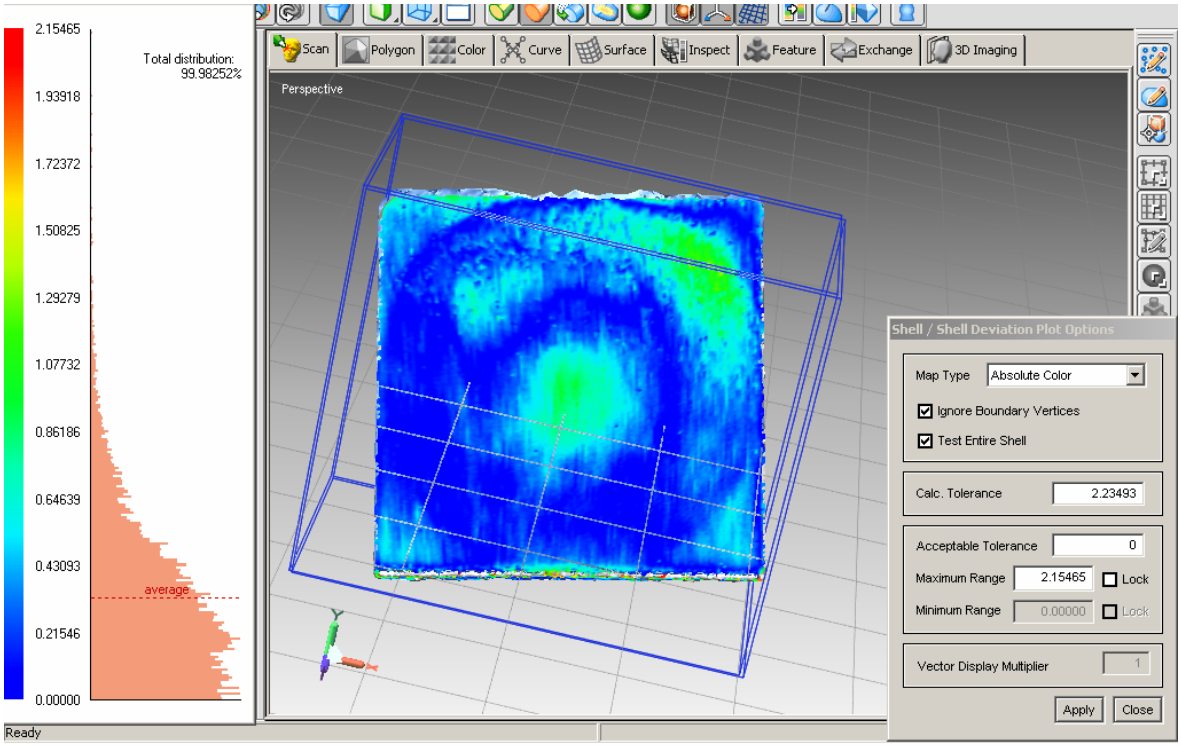

(c) part3 (unit: mm)

Figure 5-12 the difference maps of the finished parts and the parts made without the anomalies for the three parts

5.5 Conclusion

This paper presented a new, layer-based path planning strategy for material removal that can search for and remove surface anomalies without knowing their exact location, shape or size. The systems force feedback method can be modified for use with a variety of materials, and also provides a safe method of traversing the surface without tool damage. This strategy is very effective for an autonomous operation since, other than a working boundary, no other information needs to be known and no programming codes need to be changed before

machining. The method has been tested using simulation and in a test case using a 3-axis prototype grinding system. Future work should implement the system in a grinding scenario.

References:

Jung, Seul; Hsia, T.C. and Bonitz, Robert G.. (2004) "Force Tracking Impedance Control of Robot Manipulators Under Unknown Environment." *IEEE Transaction on Control Systems Technology*. (v12, n3), pp474-483

Narayanaswami, Ranga; Pang, Junhua (2003). "Multiresolution analysis as an approach for tool path planning in NC machining" CAD Computer Aided Design, v 35, n 2, February, p 167-178

Wang, Danni; Peters, Frank and Frank, Matthew (2007). "A simple points sampling strategy for unknown surface patch approximation". unpublished

Yang, S.-H.; Lee, S.-G. (2002) "CNC tool-path planning for high-speed high-resolution machining using a new tool-path calculation algorithm" International Journal of Advanced Manufacturing Technology, v 20, n 5, p 326-333

Yin, Yuehong; Hu, Hui and Xia, Yanchun. (2004) "Active tracking of unknown surface using force sensing and control technique for robot." *Sensors and Actuators, A: Physical*, (v112, n2-3), pp313-319

CHAPTER 6. IMPLEMENTATION AND VERIFICATION

6.1 Implementation

This section details the methods that were not discussed in the previous chapters but are important for the automatic material removal system.

6.1.1 System Structure

Figure 6-1 shows the structure of the automatic grinding system. The human operator uses a joystick to interface with the machine via the computer. The control algorithm combines the commands from the operator and the feedback from the sensors to decide the movement of the machine to perform appropriate grinding.

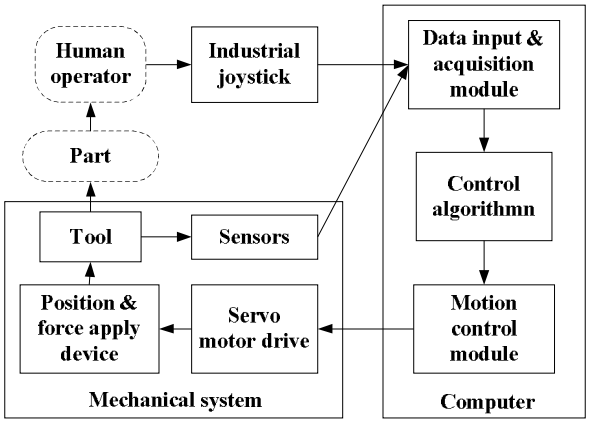

Figure 6-1 Structure of the automatic System

The mechanical system is comprised of a three axes gantry system, which corresponds to three degrees of freedom in the x, y, and z axes. Another degree of freedom is added to allow the grinder to rotate about the z axis, which is used to set up the orientation of the

grinder. The movements of the system are driven by servomotors. The position and force application device is attached to the gantry system.

The joystick should have all the control buttons for the system, since it is the primary operator interface with the system.

1) Movement control: The joystick can move the gantry system along the x, y and z axes, or rotate the grinder about the z axis.

2) Control mode switch: It is used to switch the system between automatic mode and manual mode.

3) Recording: After moving the probe to the desired locations of each boundary point, a button can be used to tell the computer to record it.

4) Start: After setting up the work and pushing the "start" button, the machine will automatically sample the reference points and work on the designated area automatically.

5) Emergency stop button.

Via the data input and acquisition module, the computer will receive commands from the joystick and read the sensors. The computer program should be able to analyze the inputs and the real-time feedback signals from the sensors, and based on the working mode and the control algorithm, generate proper signals to control the axes through the motion control module. The computer program should provide a set of steps and hints to guide the operator through the input process.

6.1.2 Mechanical system analysis

The mechanical part of the system is a gantry system driven by the servo motors. A spring and damper system is used to apply the vertical force. The mathematical functions are as follows:

$$J\ddot{\theta} + B\dot{\theta} = N\frac{K_m}{R_m}V_{in} - T \qquad (6-1)$$

$$T_z = K \bullet f + C \qquad (6-2)$$

$$f = K_s \bullet x_z + b \bullet \dot{x}_z \qquad (6-3)$$

$$x_z = z_n + L - z_r \qquad (6-4)$$

$$z_n = K_b^{-1} \bullet \theta \qquad (6-5)$$

$$\dot{x}_z \approx \dot{z}_n - \dot{z}_r \qquad (6-6)$$

where:

J the moment of inertia of the motor and load referred to the motor shaft;
θ the angular displacement of the motor shaft.
B the viscous-friction coefficient of the motor and load referred to the motor shaft;
N the gain from the gear train;
K_m motor parameter
R_m motor parameter
T the working load on this axis.
T_z the working load of the motor for the Z axis
K the gain parameter of the drive screw
C a constant of this drive screw.
f the force applied on the spring and the drive screw
K_s the spring coefficient
x_z the displacement of the spring
z_r the real position of the end of the tool.
L the constant length from the nut to the end of the tool when there is no force applied on the spring.
b the damping coefficient.
K_b the coefficient that equals to2π divided by the pitch of the axis
Z_n the position of the nut

Equation 6-1 is a motor equation. Equations 6-2 to 6-6 are for the Z axis only. Equation 6-2 is the equation for the drive screw. Equation 6-3 is for the spring and damper system. Because the system is constrained and not allowed for free vibration, and the acceleration is small, so it is neglected. The positive direction of z and x_z are pointing downward. Equation 6-4 connects the movement of the nut with the movement of the end of the tool. Equation 6-5 is the connection between the linear displacement of the nut and the angular displacement of the motor. Equation 6-6 is the differentiation of equation 6-4.

Substituting the equations, the equation for the Z axis is:

$$J\ddot{\theta}+(B+K\cdot b\cdot K_b^{-1})\dot{\theta}+K\cdot K_s\cdot K_b^{-1}\cdot\theta=N\frac{K_m}{R_m}V_{in}-C-K\cdot K_s\cdot L+K\cdot K_s\cdot z_r \qquad (6-7)$$

$$z_n=K_b^{-1}\bullet\theta \qquad (6-8)$$

Equation 6-7 and 6-8 show that on the Z axis, the displacement of the nut is affected by the input voltage and the real surface.

There is no precise mathematical model that is independent of material for the grinding process in the literature, because grinding is a very complicated process with many small cutting edges. There are some experiential models, with different parameters for different wheel and part materials. But some general rules do hold for all grinding process:

- If all other conditions are kept constant (such as the contact area), the larger the normal force is, the larger the depth of cut is.
- If all other conditions are kept constant, the smaller the feed rate is, the larger the depth of cut is.

6.1.3 Position and Force application device

Figure 6-2 shows the design of the position and force application device and the one actually used in the prototype. This device is mounted on the gantry system with movement on the x, y and z axes.

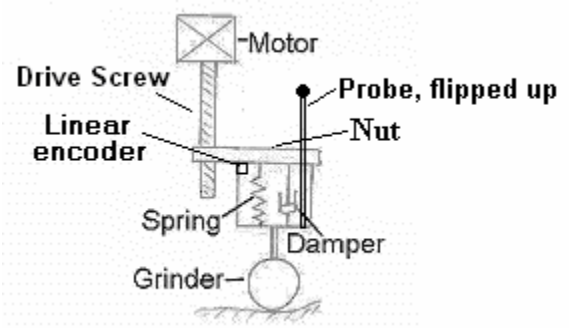

Figure 6-2 Position control and force application device for the prototype

In the design, the compression spring can be controlled to generate the desired force on the part surface according to Hooke's law. The other components are a damper to reduce vibration of the system, and a linear encoder to measure the deflection of the spring that can be used to calculate the actual force applied. The spring is compressed in a housing initially, and with the constraint of the housing the spring can only be compressed more. This device can only provide vertical force, so the anomalies should be positioned generally facing up to get better material removal results. A probe is also attached to the device. When it is flipped down, it is used to sample the boundary and reference points; it will be flipped up during grinding.

6.1.4 Motion control

In material removal processes, three basic variables should be controlled properly: the position, the feed rate (velocity) and the cutting force.

In cleaning room grinding, wheel speed, feed rate and grinding force are important parameters that influence the depth of cut and material removal rate significantly (AFS 1977). In this dissertation, the wheel speed is assumed to be constant, while the grinding force will be monitored and kept within a range, and the feed rate will be controlled.

The grinding force can be split into three components, as shown in Figure 6-3. (Marinescu 2004) The tangent force F_t acts tangentially to the abrasive tool surface and the surface velocity of the wheel. It is responsible for power dissipation. The side force F_a is perpendicular to both the tangential and normal forces. It arises when there is a sideways movement of the wheel. The normal force F_n is perpendicular to the grinding surface. It is usually much larger than the other two forces and is the most important factor in material removal. A lower normal force will result in less depth of cut.

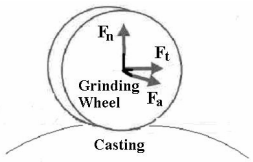

Figure 6-3 Grinding force components (Marinescu 2004)

6.1.4.1 The control strategy in the manual mode

In the manual mode, the position control is taken over by the operator via a joystick. However, the system is still responsible for maintaining the proper cutting force and feed rate.

Both the force and the feed rate are kept constant. To remove more material from a certain spot, the operator can move the grinder back and forth repeatedly.

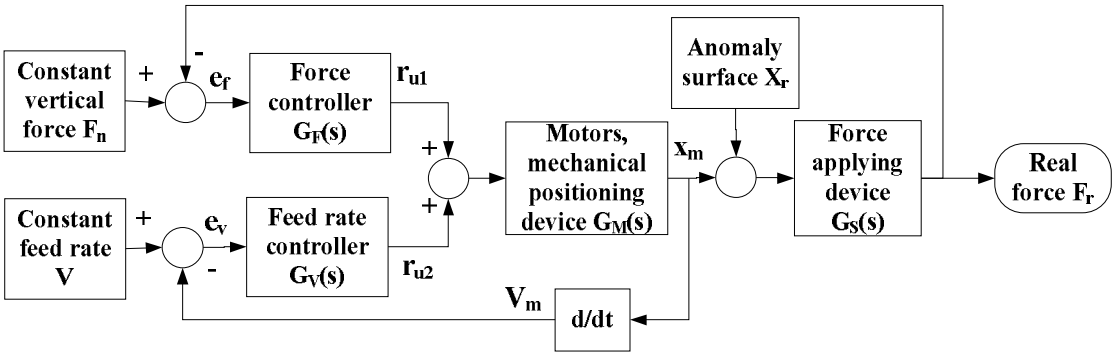

Figure 6-4 The control strategy in manual mode

In Figure 6-4:

F_n the force to be kept constant;
e_f the force error;
r_{u1} the output of the force controller and part of the voltage input of the motors;
x_m the position of the positioning motor;
x_r the real surface, which is unknown and can be looked as the system disturbance, and works together with x_r as the input of the force application device to decide how much force is applied on the grinding surface.
$G_M(s)$ the transfer function of the mechanical system;
$G_S(s)$ the transfer function of the force application device;
V the feed rate value to be kept constant;
e_V the feed rate error;
r_{u2} the output of the force controller and the part of the voltage input of the motors;
V_m the real feed rate.

As shown in Figure 6-4, this is a constant input control system. The change in force caused by the anomaly can be considered as a disturbance. Section 6.1.3 shows that the force application device is a spring damping system, so the force is only determined by the deflection of the spring. As long as the spring coefficient K_s is set, it will follow equation 6-3 without being affected by the material change of the cutting tool or part.

PID controllers can be used to maintain constant output. Since there is no parameters that will change with the material properties, the controller will only need to be tuned once. The force controller $G_F(s)$ and the feed rate controller $G_V(s)$ are both designed to be PID controllers.

$$G_F(s) = K_{pF}(1 + \frac{1}{T_{IF}s} + T_{DF}s)$$

$$G_V(s) = K_{pV}(1 + \frac{1}{T_{IV}s} + T_{DV}s)$$

The PID parameters K_{pF}, T_{IF}, T_{DF}, K_{pV}, T_{IV}, and T_{DV} will be decided according to the system transfer functions.

6.1.4.2 The control strategy in the automatic mode

The goal of this grinding process is to remove excess material contained within the anomaly boundary points and make the surface smooth. The tool must be able to follow the approximated surface as precisely as possible.

From the path planning strategy described in chapter 5, for layers higher than layer 1, it is obvious that the most efficient way to finish the job is to grind at high speed and high MRR (material removal rate). It doesn't matter if there is considerable error between the ground surface and the reference surface in the current layer, because it won't be the final surface. But the grinding force has to be controlled within an operating range (F_{min} to F_{max}) to assure effective material removal and to prevent wheel breakage. It is reasonable to apply precise position control only in layer 1 as a finish machining process to achieve the

approximated surface. Since a different feed rate and/or grinding force will result in different depths of cut and finished surface, they have to be controlled more precisely in layer 1 than in other layers.

1) The control strategy in layer 1

In order to create the approximated surface precisely, the amount of material removed has to be adjusted constantly. There are two ways to change the amount of material removed in one pass, either by controlling the normal force or the feed rate.

In force control, the feed rate is kept constant all the time by the controller. The force controller should be able to calculate the force needed to create the approximated surface based on the difference between the ground surface and the approximated surface, and apply the desired force effectively. The depth of cut is proportional to the normal force under a fixed feed rate, so the needed force can be calculated accordingly. However, the depth of cut is dependant on the material properties, so it should be given from experimental results.

In feed rate control, the force is monitored and kept within a range but not specially controlled. If the real force is larger than the maximum force (found from experiments), the tool will be moved to an upper layer according to the path planning strategy. The difference of the ground surface and the approximated surface is the inputted to the feed rate controller to calculate the feed rate that the system needed to create the desired surface. If the difference of the surfaces shows that there is more material to be removed, the feed rate will be reduced.

If there is less material to remove, the feed rate will be increased, otherwise it will be kept at the current value.

For layer 1, the feed rate control would calculate the needed federate based on the difference of the true surface and the reference surface, avoiding the influence of different material properties (both the material of the casting and the grinding wheel), and the condition of the grinding wheel. The force control is more complicated. The changing force is calculated based on the amount of material to be removed and is directly connected with the material properties and wheel condition. Experiments will be required to test the material removal rate in different feed rate for different combinations of grinding wheel and casting materials. The parameters in the controller would also need to be tuned for different material combinations. In addition, when increasing the cutting force, the increased force might exceed the maximum force and the grinder will be moved to an upper layer, making the process more complicated. So in layer 1, the feed rate control is used in this dissertation to make the strategy general. The strategy is shown in Figure 6-5. It includes a velocity feedback inner loop and a position feedback outer loop.

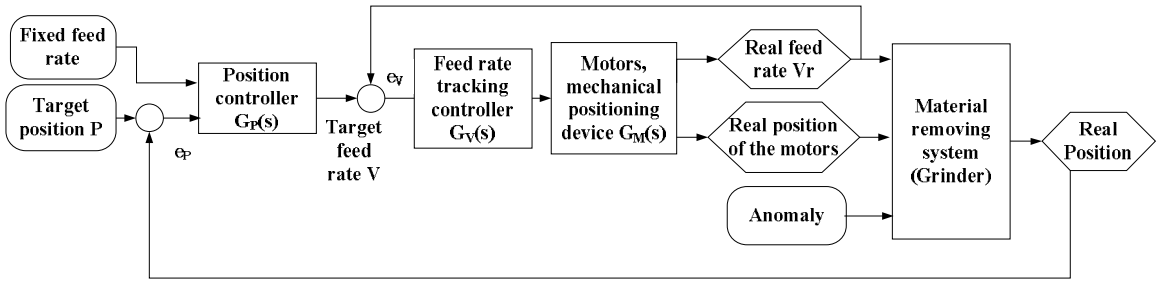

Figure 6-5 The control strategy in layer 1

The feed rate controller in the inner loop needs to ensure that the system's real feed rate can follow the target feed rate exactly with small settling time. It can be subtracted as a sub-system with a changing load. The controller will try to follow the input no matter what the working load is. Feed forward compensator (FFC) has been well studied and constantly used with a PID controller to reduce the tracking error in a tracking system.

The position controller in the outer loop should be able to calculate the target feed rate according to the sensor feed back about the real position. A traditional PID controller with a FFC can also be tuned to track the position input.

2) The control strategy in layers above layer 1

A constant high feed rate is used to achieve a high MRR in layers above layer 1. However, for a positioning system with a spring working on a surface with unknown anomalies, a constant feed rate and precise positioning are contradictory to each other because the anomaly surface varies from the reference surface. Fortunately, in layers above layer 1, as long as the grinding wheel is working within a proper grinding force range, reaching a precise position is not as important as getting rid of the excess material as quickly as possible. The remaining material will be ground off the next time the grinder passes. Therefore, the control strategy in layers above layer 1 is a relatively loose control strategy, as described below.

a) The feed rate is kept at a constant higher value (around 1 inch/s based on observations in steel foundries).

b) Grinding force is monitored during this process. As long as the force is within an experiential range (typically from 20-60 pounds), the system is an open loop system. No additional adjustments will be made according to the difference between the target position and the real position. Otherwise, the target position will change to an upper or lower layer according to the path planning strategy.

This strategy is shown in figure 6-6.

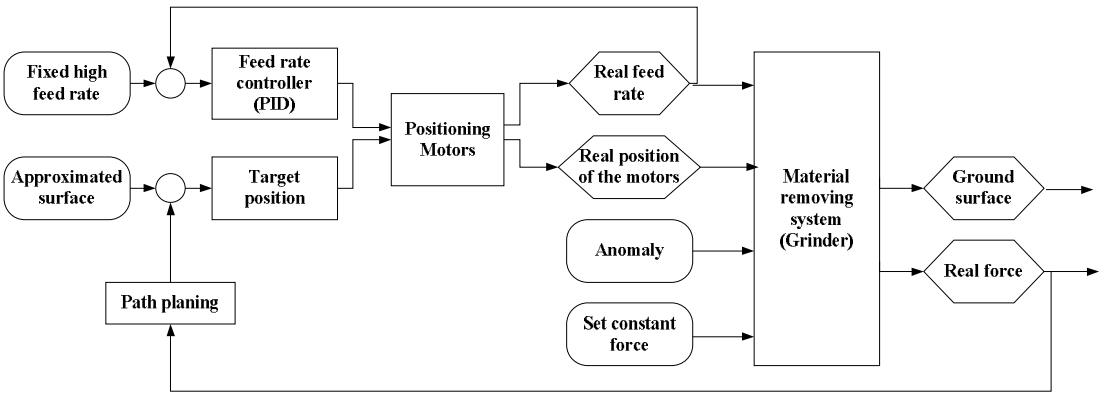

Figure 6-6 The control strategy in layers above layer 1

Similar to the manual control, this is a constant feed rate control. A PID controller is used to make sure that the feed rate is kept at the fixed value.

6.2 Verification

A physical prototype was made to verify the automatic material removal methods and algorithms in this dissertation. The manual mode was not implemented in this system. The feed rate control in layer 1 was not implemented either, so multiple iterations in layer 1 were noticed instead of the only one iteration designed with the feed rate control. But that does not affect the path planning algorithm, because the system will only stop in layer 1 when the designated surface tolerance was met.

In the prototype, a Gantry III system with servomotors from Techno Inc. was used, with a travel distance of 13.7'' by 11.4'' by 6.8''. A small fixture of 3'' by 3'' was used to keep the parts in position, and the setting of the orientation angle was achieved by manually rotating the fixture instead of rotating the grinder. The NI motion control card PCI-7350 was used to drive the servo motor to the target position on the reference surfaces. It has a built in velocity control that can keep the feed rate to a designated constant value and its input channels work like a basic data acquisition module. The NI motor power drive MID-7654/2 was used to convert the commands from the motion control card to the voltage signals that actually move the servomotors. Figure 6-7 shows a picture of the gantry system, the NI servo motor drive and the fixture.

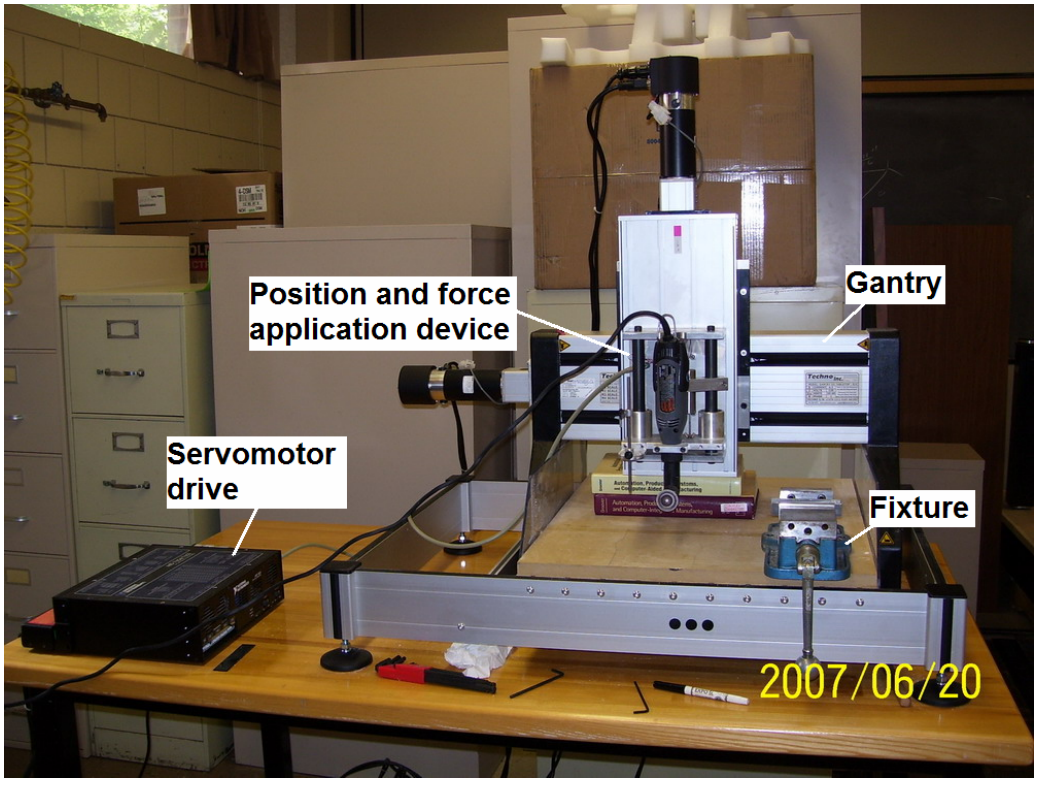

Figure 6-7 The gantry III system, the servomotor drive and the fixture

The prototype changed the design of the position and force application device a little bit to fit the limit of the Dremel tool used. (Figure 6-8) The Dremel tool used as the grinder is not powerful enough to bear the 60 lbs force in the initial design; it can only afford a force at around 0.5 lbs before stopping the wheel. Since the weight of the moving part of the device has exceeded the 0.5 lbs limit, the spring is put underneath the moving part. However, the calculation method for the force stays the same, so it will still be able to verify the strategies in this dissertation. The damper was also not needed in this prototype system. A Schaevitz LC500 Linear Variable Digital Transducer (LVDT) was used to measure the deflection of the spring.

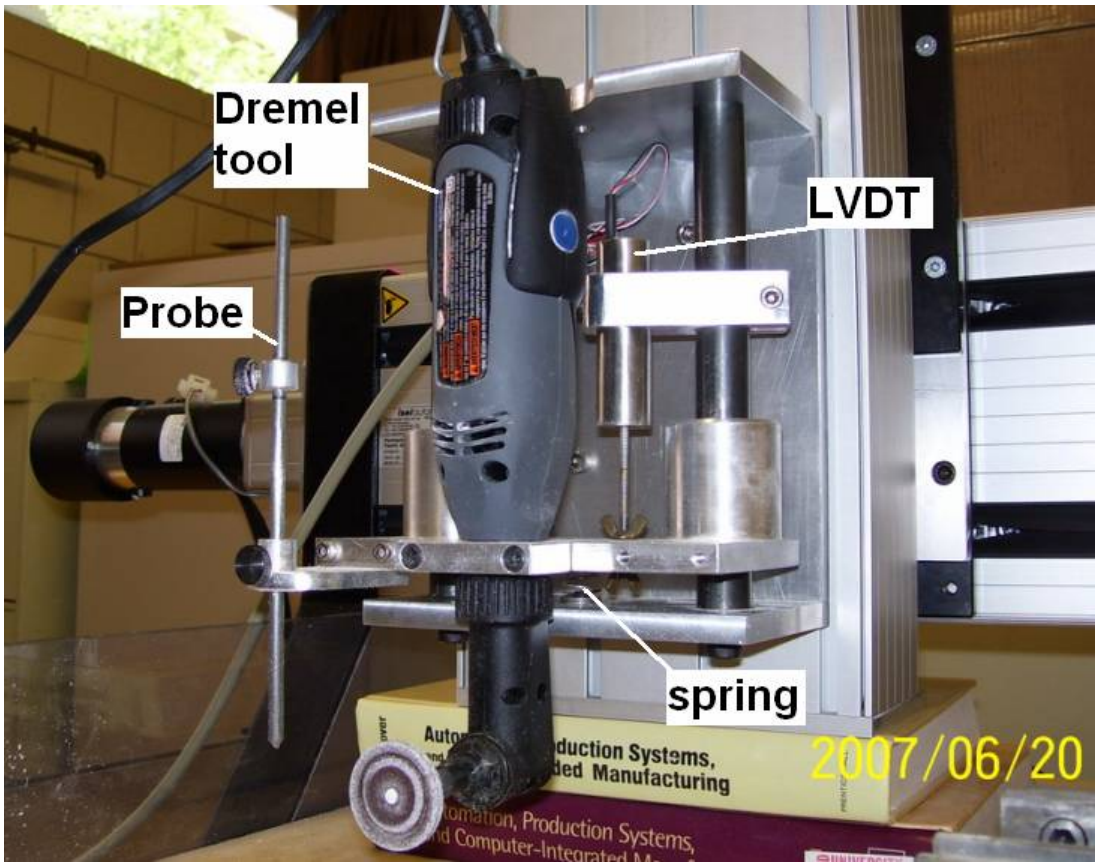

Figure 6-8 The position and force application device in the prototype

Buttons from the computer program interface were used to control the movements of the axes instead of using a joystick. The computer interface provides the interface for all the necessary inputs, and after hitting the start button, the program will automatically sample surface points based on the anomaly and sampling boundary points using the simple point sampling strategy in chapter 4. This is followed by the automatic removal of the anomalies using the path planning strategy in chapter 5. Figure 6-9 shows the computer program interface.

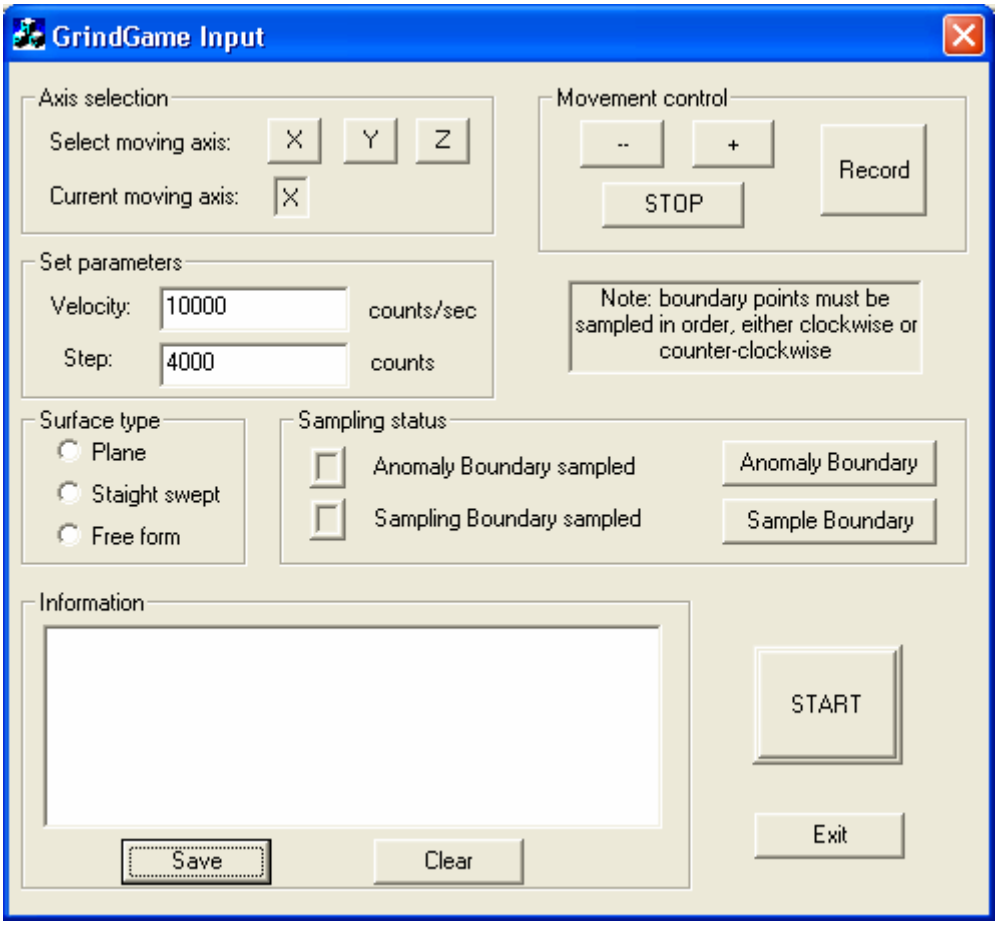

Figure 6-9 The computer program interface

Three surface samples with anomalies made with epoxy were tested. They were:

1) A flat surface with a sloped “H” anomaly (Figure 6-10 (a));
2) A concave cylindrical surface with a “selected radio button” anomalies (Figure 6-10 (b));
3) A convex spherical surface with two separated irregular shaped anomalies (Figure 6-10 (c)).

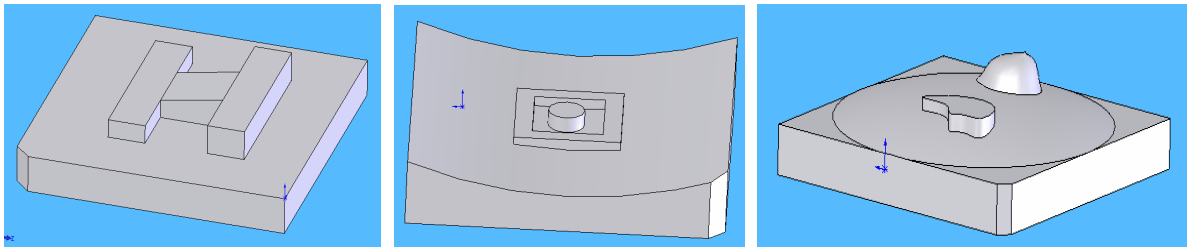

(a) (b) (c)

Figure 6-10 CAD models of the parts with the anomalies

The parts were laser scanned after the automatic grinding operation, as well as the printed parts without the anomalies. The reverse engineering software Rapidform was used to reconstruct the surfaces, and the surfaces after grinding were compared to the corresponding surfaces of the part without the anomalies. Figure 6-11 shows the epoxy parts before and after the automatic grinding operation. The total time including sampling used for the three parts was 32 minutes, 15 minutes and 27 minutes respectively.

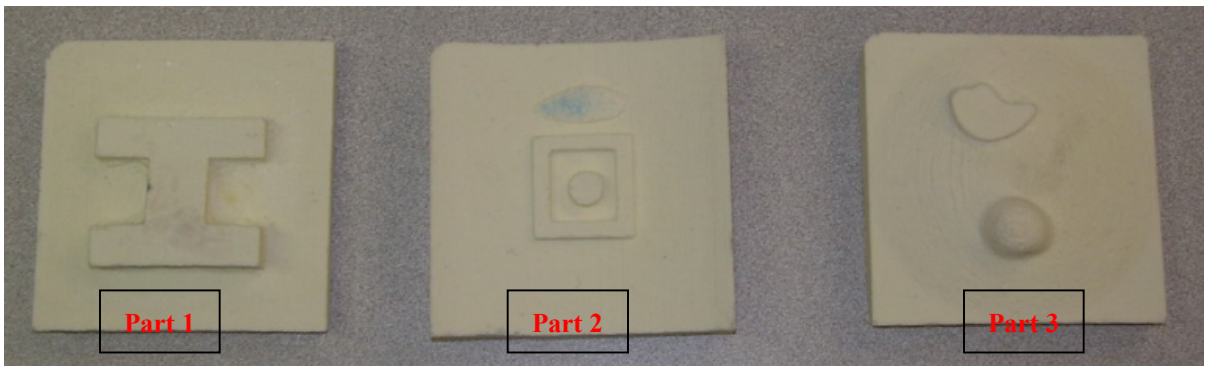

(a) parts before grinding

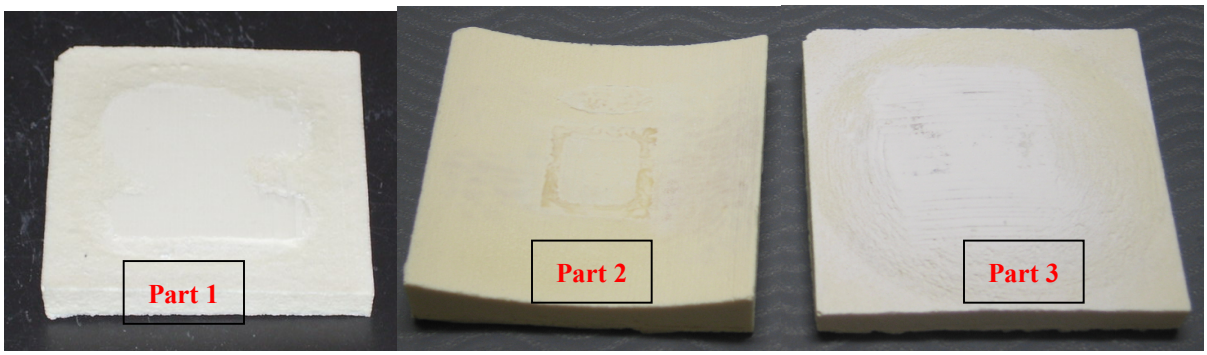

(b) parts after grinding

Figure 6-11 the parts before and after the automatic grinding operation

Figure 6-12 shows the difference map of the scanned finished part and the scanned part without the anomalies.

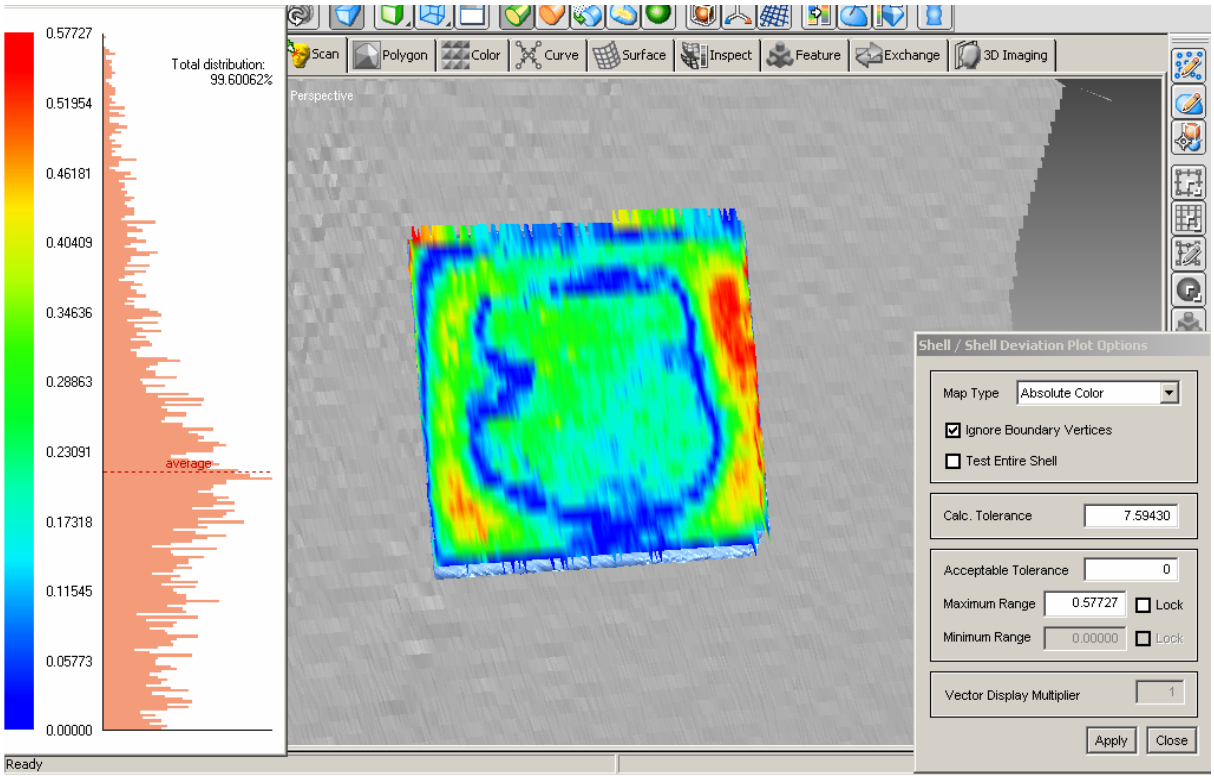

(a) part 1

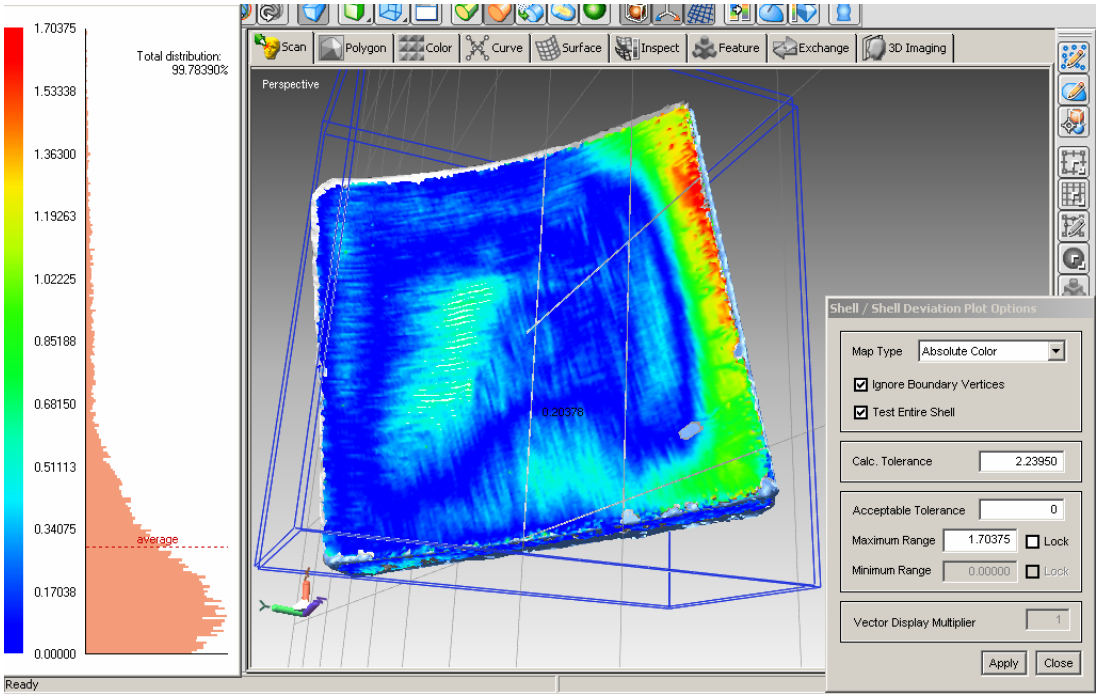

(b) part 2

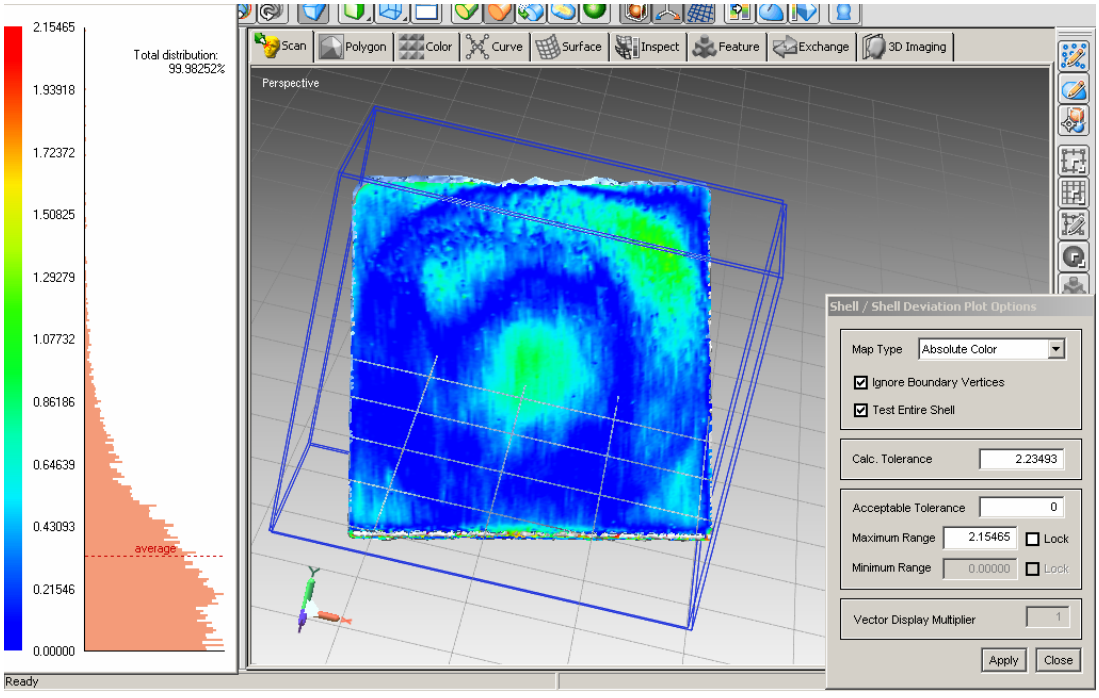

(c) part3

Figure 6-12 the difference map of the scanned finished part and the original CAD model without the anomalies (unit: mm)

As can be seem from the maps, the difference of the finished surface and the CAD model are at an average of 0.3 mm (0.012inches). Surface areas with the biggest difference in the maps are actually not in the defined anomaly boundaries. This proves that the surface sampling method and the path planning method is effective.

Additional analyses were done for the flatness of the ground part 1 and the cylindricity of the ground part 2. The flatness of part 1 was 0.89945mm and the cylindricity of part 2 was 0.92623mm. From the result, it can be seen that the ground surfaces satisfy the requirements in the cleaning room grinding application. Therefore, the strategy in this dissertation was verified.

The sources of error in the system and in the experiments were:

1) The patterns and compare parts have errors. They were printed from a 3D printing rapid prototyping machine, which was not in its best working condition and with its system error.

2) The epoxy parts made from the model have error due to the casting procedure.

3) The laser scanner has measuring error.

4) The surface registration error.

5) The gantry system has following error.

6) The LVDT has measurement error.

7) The sampled points have measurement error.

8) The Surface approximation error.

9) The error caused by tool geometry and accessibility.

CHAPTER 7. GENERAL CONCLUSION

7.1 Conclusion

The current material removal method for unknown objects is inefficient and not ergonomic. However, the process is not well studied. For example, mechanization of cleaning room grinding is needed to improve efficiency when producing low volume products, which are particularly prevalent in the steel casting industry. Current automatic machines are not able to accommodate grinding of unexpected anomalies.

In this dissertation, the characteristics of cleaning room grinding problems were investigated. An automatic grinding system was designed to solve this problem. This system includes deciding and gathering necessary information from the objects and performing necessary data preparations. A simple point sampling strategy was developed as well as the surface approximation method to guide the system to sample an adequate number of points in some specific locations to get a good fit. The approximation surface was used as the reference surface in the machining process. A layer-based path planning logic was developed to divide the anomalies into layers, and together with a selected hybrid position and force/velocity control method, the path planning strategy was able to guide the tool among the layers within the designated working area with constant contact with the anomalies. The path planning strategy is also universal to all objects and anomalies; no programming codes need to be changed for different part. The implementation of a proposed automatic grinding

machine was illustrated and the process and path planning strategies were verified to be effective and efficient.

The application of this general material removal strategy can also be extended into any area with an unknown stock or environment while a specific surface needs to be created.

7.2 Future work

Future work will include:

1) Search for the optimum points sampling strategy; search for the sampling strategy for more complicated surfaces.

2) Implement the manual mode and test the control strategy for it.

3) Implement and test the controllers for the feed rate control in layer one, and use the one that is most robust for different materials.

4) Design and carry out the experiments for finding the proper values of Fmax and Fmin for different combination of tool and part materials.

5) Constructing the full-scale machine and testing with metal castings.

REFERENCES

AFS. (1977) "Cleaning castings." *American Foundry Men's Society, inc.*

Chen, Seng-Chi and Tung, Pi-Cheng. (2000) "Trajectory planning for automated robotic deburring on an unknown contour." *International journal of machine tools & manufacture*, (v40, n7), pp957-978

Dimo, H.O.; Jin, Dewen; Zhang, Jichuan and Gruver, William A.. (2001) "Vibration control of a redundant robot for grinding." *Proceedings of the IEEE International Conference on Systems, Man and Cybernetics*, (v1), pp389-394

Erlbacher, Edwin A.. (2000) "Force control basics." *Industrial Robot: An International Journal.* (v27, n1), pp20-29

Geomagic Inc. (2007) "3D Scanners Report", http://www.geomagic.com/en/dssp_resources/scanners/3d_scanner_report.pdf

Hogan, N. (1985) "Impedence control: An approach to manipulation". *Journal of Dynamic Syst., Measurement Contr.*, vol. 107, Mar., pp. 1-24

Iwasaki, Masahiro; Tsujiuchi, Nobutaka and Koizumi, Takayuki. (2003). "Adaptive force control for unknown environment using skidding mode controller with variable hyperplane". *JSME International Journal.* Series C, vol. 46, No. 3. pp.967-972

Jung, Seul; Hsia, T.C. and Bonitz, Robert G.. (2004) "Force Tracking Impedance Control of Robot Manipulators Under Unknown Environment." *IEEE Transaction on Control Systems Technology*. (v12, n3), pp474-483

Kiguchi, Kazuo and Fukuda, Toshio. (2000) "Position/Force Control of Robot Manipulators for Geometrically Unknown Objects Using Fuzzy Neural Networks." *IEEE Transaction on Industrial Electronics*. (v47, n3), pp641-649

Kuo, R.J. (1997) "A robotic die polishing system through fuzzy neural networks". *Comput*. Ind. 32, pp. 273–280.

Li, Y F and Liu, Z G. (2003) "Method for determining the probing points for efficient measurement and reconstruction of freeform surfaces". *MEASUREMENT SCIENCE AND TECHNOLOGY*. (v14), pp1280-1288

Marinescu, Ioan D. (2004) "Tribology of abrasive machining processes". William Andrew Publication, pp123

Mitchell, M.; Forrest, S. and Holland, J. H. (1992). "The royal road for genetic algorithms: Fitness landscapes and GA performance". *Proceedings of the First European Conference on Artificial Life*. Cambridge, MA: MIT Press. pp 245-254

Nandi, Arup Kumar and Pratihar, Dilip Kumar. (2004) "Automatic design of fuzzy logic controller using a genetic algorithm—to predict power requirement and surface finish in grinding." *Journal of Materials Processing Technology*. (v148, n3), pp288–300

Pagilla, P.R.; Yu, B. (2001) "Adaptive control of robotic surface finishing processes." *Proceedings of the American Control Conference.* (v1), pp 630-635

Piegl, Les and Tiller, Wayne. "The NURBS Book", 2nd edition, Springer, 1997

Prabhakar, R. Pagilla and Yu, B.. (2001). "Adaptive Control of Robotic Surface Finishing Processes." *Proceedings of the American Control Conference*. (v1), pp630-635

Raibert, M. and Craig, J.. "Hybrid position/force control of manipulators". J. Dynamic Syst., Mesearment Contr.. vol 103, Feb, no.2, pp. 126-133

Roy, Jaydeep and Whitcomb, Louis L.. (2002). "Adaptive force control of position/velocity controlled robots: theory and experiment". *IEEE Transaction on Robotics and Automation.* Vol. 18, No. 2, April. pp.121-137

Shannon, C. E. (1949), "Communication in the presence of noise", *Proc. Institute of Radio Engineers*, vol. 37, no.1, pp. 10-21.

T. Yoshikawa. (2000) "Force control of robot manipulators", *Proc. IEEE Int. Conf. Robotics and Automation,* (vol.1), pp.220-226

Thomessen, Trygve; Lien, T.K.; and Sannaes, P.K.. (2001) "Robot control system for grinding of large hydro power turbines." *Industrial Robot: An International Journal.* (v28, n4), pp328-334

Wang, Y.T. and Jan, Y.J.. (2000) "A Robot-Assisted Finishing System with an Active Torque Controller." *Proceedings of the 2000 IEEE International Conference on Robotics & Automation.* (San Francisco, CA, April), pp1568-1573

Wu, Shuning and Olafsson, Sigurdur. (2006) "Optimal Instance Selection for Improved Decision Trees". *Preliminary proposal,* pp 7-9

Yin, Yuehong; Hu, Hui and Xia, Yanchun. (2004) "Active tracking of unknown surface using force sensing and control technique for robot." *Sensors and Actuators, A: Physical*, (v112, n2-3), pp313-319

ACKNOWLEDGEMENTS

The work with this dissertation has been interesting and challenging. My sincere appreciation goes to several persons for their support, instruction and encouragement.

First of all, I would like to take this opportunity to extend my deepest gratitude to my advisors, Dr. Frank Peters and Dr. Matthew Frank, for their inspiring way to guide me to a deeper understanding of the knowledge on material removal strategies. Dr. Peters provides me with great details of the unknown material removal problem in the metalcasting grinding operation; the discussions with Dr. Frank are always productive and innovative. Without the help of them, I wouldn't be able to finish this dissertation. I am also grateful to the other professors in my academic committee. The informative advice and questions from the professors have been instrumental and crucial in the progress of my research. My sincere appreciation also goes to Kevin Brownfield and Mike Renze, for helping me build and trouble shooting the hardware so that I can finish my experiments in such a short time.

My gratitude also goes to other staff, students and colleagues at the Department of Industrial Engineering for developing a good working atmosphere, especially Brian Harwood, Xiaoming Luo, Fanqi Meng and Lei Yu, for their assistance and companionships throughout my work.

Last but not least, I am greatly grateful to my husband, my lovely little daughter and my family for their understanding, patience and support during the entire period of my study.